

Infinite Mixtures of Infinite Factor Analysers

Keefe Murphy^{1, 2}, Isobel Claire Gormley^{1, 2}, and Cinzia Viroli³

¹School of Mathematics and Statistics, University College Dublin

²Insight Centre for Data Analytics, University College Dublin

³Department of Statistical Sciences, University of Bologna

Abstract

Factor-analytic Gaussian mixture models are often employed as a model-based approach to clustering high-dimensional data. Typically, the numbers of clusters and latent factors must be specified in advance of model fitting, and remain fixed. The pair which optimises some model selection criterion is then chosen. For computational reasons, models in which the number of latent factors is common across clusters are generally considered.

Here the infinite mixture of infinite factor analysers (IMIFA) model is introduced. IMIFA employs a Poisson-Dirichlet process prior to facilitate automatic inference of the number of clusters using the stick-breaking construction and a slice sampler. Furthermore, IMIFA employs shrinkage priors to allow cluster-specific numbers of factors, automatically inferred via an adaptive Gibbs sampler. IMIFA is presented as the flagship of a family of factor-analytic mixture models, providing flexible approaches to clustering high-dimensional data.

A simulation study and applications to a benchmark data set, metabolomic spectral data, and a manifold learning handwritten digit example illustrate the IMIFA model and its advantageous features: IMIFA obviates the need for model selection criteria, reduces model search and the associated computational burden, improves clustering performance by allowing cluster-specific numbers of factors, and quantifies uncertainty in the numbers of clusters and cluster-specific factors.

1 Introduction

Modern clustering problems are becoming increasingly high-dimensional in nature, in the sense that p , the number of variables, may be comparable to or even greater than N , the number of observations to be clustered. In such cases, many common clustering techniques tend to perform poorly, or may even be intractable.

Factor analysis (Knott & Bartholomew, 1999) is a traditional, well known approach to parsimoniously modelling data, often employed for dimension reduction; Bai & Li (2012) outline some computational difficulties which arise specifically when $N \ll p$. Model-based clustering methods which rely on such latent factor models have long been successfully utilised to cluster high-dimensional data. For example, Ghahramani & Hinton (1996) propose a mixture of factor analysers model (MFA) with a cluster-specific parsimonious covariance matrix and estimate it via an EM algorithm; McLachlan &

Peel (2000) provide a succinct overview. Estimation of MFA models has also been considered in a Bayesian framework (Diebolt & Robert, 1994; Richardson & Green, 1997; Fokoué & Titterton, 2003). McNicholas & Murphy (2008) develop a suite of similar parsimonious Gaussian mixture models. Other related developments in this area include Baek et al. (2010) and Viroli (2010), among others.

Using a MFA model for clustering purposes typically requires specification of the number of clusters and the number of factors in advance of model fitting. In what follows the number of clusters and number of components in a mixture model are assumed to be equal, although this is not always the case (Hennig, 2010). Generally, a range of MFA models with different fixed numbers of clusters and factors are fitted. In order to highlight the optimal model the fitted models are compared through the use of information criteria such as the Bayesian Information Criterion (BIC) (Kass & Raftery, 1995), Akaike’s Information Criterion (AIC) (Schwarz, 1978), or the Deviance Information Criterion (Spiegelhalter et al., 2002, 2014). Within a Bayesian framework Fokoué & Titterton (2003) use a stochastic model selection approach, invoking a birth-death MCMC algorithm (Stephens, 2000), but do not simultaneously choose the optimal number of clusters and number of factors.

Conducting an exhaustive search of the model space is computationally expensive; the cost is typically reduced by only considering models in which the number of factors is common across clusters. Regardless, even searching the reduced model space is still a computationally onerous task. The problem of choosing the optimal model is further exacerbated by the fraught task of choosing among the range of information criteria and model selection tools available, which often suggest different optimal models. Moreover, enforcing the common number of factors across clusters constraint may lead to poor clustering performance due to the lack of flexibility afforded by such a model.

The infinite mixture of infinite factor analysers (IMIFA) model is introduced here which theoretically allows infinitely many clusters and simultaneously infinitely many factors within each cluster. IMIFA relies on an infinite mixture model through the use of a nonparametric Poisson-Dirichlet process prior (Perman et al., 1992; Pitman & Yor, 1997), of which the well-known Dirichlet process (Ferguson, 1973) is a special case. The infinite mixture model framework allows the number of clusters present to be automatically inferred; here the stick-breaking construction (Sethuraman, 1994) and an independent slice-efficient sampler (Kalli et al., 2011) are employed to facilitate this.

Furthermore, IMIFA addresses the difficulty in choosing the optimal number of factors, and facilitates more flexible factor-analytic models in which the number of factors may be cluster-specific, by allowing infinitely many factors within each cluster. This is achieved by assuming a multiplicative gamma process (MGP) shrinkage prior (Bhattacharya & Dunson, 2011; Durante, 2017) on the cluster-specific factor loading matrices. Such a prior posits infinitely many factors within each cluster and allows the degree of shrinkage of the factor loadings towards zero to increase as the factor number tends towards infinity. The number of factors with non-negligible loadings can be considered as the ‘active’ number of factors within each cluster. Following Bhattacharya & Dunson (2011), an efficient, adaptive Gibbs sampling algorithm is employed for estimation. Thus the choice of the number of active factors is automated, and model flexibility is greatly enhanced by allowing different numbers of active factors in different clusters.

IMIFA therefore theoretically allows infinitely many clusters and simultaneously infinitely many factors within each cluster, offering a single-pass, computationally efficient

approach to clustering high-dimensional data. Fitting an IMIFA model estimates, and quantifies the uncertainty in, the optimal number of non-empty clusters and the optimal numbers of cluster-specific factors, entirely obviating the need to select and employ a model selection criterion, while reducing the model search, and potentially improving clustering performance through the additional modelling flexibility IMIFA affords.

IMIFA can be viewed as the most flexible and efficient flagship model at the head of a family of Bayesian factor-analytic mixture models, the most elementary of which is the well-known factor analysis model. Between these extremes, other members of the IMIFA family of models include the established MFA model and its novel extension to the finite mixture of infinite factor analysers (MIFA) model. MIFA generalises the MGP prior to combine a finite mixture with an infinite factor model and is introduced here. Overfitted factor-analytic mixtures ([van Havre et al., 2015](#)) also belong to the IMIFA family; in particular the overfitted mixture of infinite factor analysers (OMIFA) model is also introduced herein. Section 2 considers the full family of models, incrementally developing the IMIFA family hierarchy, beginning with the elementary factor analysis and MFA models and concluding with the flagship IMIFA model. Prior specifications, strategies for conducting posterior inference via MCMC, and approaches to posterior predictive model checking are provided for each model in the IMIFA family.

The remainder of the article proceeds as follows: Section 3 considers implementation of the IMIFA family of models and their performance both in terms of clustering performance and computational efficiency. The strong performance of IMIFA is comprehensively demonstrated with recourse to a thorough simulation study (Section 3.1) which explores different dimensionality scenarios. In Section 3.2 a benchmarking experiment is conducted on the well-known Italian olive oil data set, often employed as an illustrative example in factor-analytic settings, with excellent results. Section 3.3 outlines a real data application through the cluster analysis of high-dimensional spectral metabolomic data from an epilepsy study. A final convincing demonstration of IMIFA, in the context of manifold learning, is provided in Section 3.4 through application to clustering United States Postal Service handwritten digit data, a setting for which fitting sub-models from the IMIFA model would be practically infeasible. Section 4 concludes the article with a discussion of IMIFA, its related models, and thoughts on future research directions.

A software implementation for IMIFA and its family of sub-models is provided by the associated R package **IMIFA** ([Murphy et al., 2017](#)), which is freely available from www.r-project.org ([R Core Team, 2017](#)), with which all results were generated.

2 The Suite of IMIFA Related Models and their Inferential Procedures

The hierarchy of the IMIFA family of models is incrementally delineated herein, under the Bayesian paradigm, including a comprehensive review of extant methodologies, the introduction of novel sub-models of varying degrees of complexity, and concluding with the flagship IMIFA model. Initially in Section 2.1 the well known factor analysis (FA) model is detailed. Clustering capabilities are incorporated via the mixture of factor analysers (MFA) model in Section 2.2. The novel mixture of infinite factor analysers (MIFA) model, which relies on the recent infinite factor analysis (IFA) model ([Bhattacharya &](#)

Dunson, 2011), is introduced in Section 2.3. The mixture basis of these models is developed further in two separate streams: overfitted mixtures of (infinite) factor analysers (OMFA and OMIFA) in Section 2.4 and infinite mixtures of (infinite) factor analysers (IMFA and the flagship IMIFA) in Section 2.5. Prior specifications, MCMC based inferential procedures, and approaches to posterior predictive model checking are detailed; model-specific implementation issues that arise in practice are addressed. The MIFA, OMIFA, and IMIFA models are all new, novel methodologies.

2.1 Factor Analysis

Factor analysis (FA) is a Gaussian latent variable model (Knott & Bartholomew, 1999), often employed for dimension reduction. For $i = 1, \dots, N$ observations, the p -dimensional feature vector $\underline{x}_i = (x_{i1}, x_{i2}, \dots, x_{ip})^\top$, with mean $\underline{\mu}$ and covariance matrix Σ , is assumed to linearly depend on a q -vector ($q \ll p$) of common latent factors $\underline{\eta}_i$ and additional sources of variation termed specific factors $\underline{\varepsilon}_i = (\varepsilon_{i1}, \varepsilon_{i2}, \dots, \varepsilon_{ip})^\top$, via

$$\underline{x}_i - \underline{\mu} = \Lambda \underline{\eta}_i + \underline{\varepsilon}_i$$

where Λ denotes the $p \times q$ factor loadings matrix. It is assumed that $\underline{\eta}_i \sim \text{MVN}_q(\underline{0}, \mathcal{I}_q)$ where \mathcal{I}_q denotes the $q \times q$ identity matrix, and that $\underline{\varepsilon}_i \sim \text{MVN}_p(\underline{0}, \Psi)$, where Ψ is a diagonal matrix with non-zero elements ψ_1, \dots, ψ_p known as uniquenesses. Thus, marginally $\underline{x}_i \sim \text{MVN}_p(\underline{\mu}, \Sigma = \Lambda \Lambda^\top + \Psi)$ and conditionally $\underline{x}_i | \underline{\eta}_i \sim \text{MVN}_p(\underline{\mu} + \Lambda \underline{\eta}_i, \Psi)$.

2.1.1 Prior Specification and Identifiability Issues

The conjugate nature of the various priors detailed below facilitates MCMC sampling via efficient Gibbs updates. A multivariate normal prior distribution is assumed for the factor loadings of the j -th variable across the $k = 1, \dots, q$ factors: $\underline{\lambda}_j \sim \text{MVN}_q(\underline{0}, \mathcal{I}_q)$. A diffuse multivariate normal prior distribution is assumed for the mean $\underline{\mu} \sim \text{MVN}_p(\tilde{\underline{\mu}}, \varphi^{-1} \tilde{\Sigma})$ where $\tilde{\underline{\mu}}$ is given by the sample mean and $\tilde{\Sigma}$ is a diagonal matrix with non-zero entries given by the diagonal entries of the sample covariance matrix \mathbf{S} . The scalar φ controls the level of diffusion; lower values lead to a flattening of the prior and loosens the influence of its somewhat data-driven specification.

The uniquenesses are assumed to have an inverse gamma prior distribution $\psi_j \sim \text{IG}(\alpha, \beta_j)$ for $j = 1, \dots, p$. Guided by Frühwirth-Schnatter, S. and Lopes, H. F. (2010), the hyperparameters are chosen to ensure that each ψ_j is bounded away from 0, in such a way that Heywood problems are avoided, with a sufficiently large shape α and variable-specific rates derived as $\beta_j = \frac{\alpha-1}{(\mathbf{S}^{-1})_{jj}}$. Here, when idiosyncratic variances are not too unbalanced and/or in $N \ll p$ settings, constraining Ψ to be isotropic and/or instead using $\beta = (\alpha-1)/(\prod_{j=1}^p (\mathbf{S}^+)_{jj})^{1/p}$, provides parsimony with only a single rate hyperparameter, where \mathbf{S}^+ is the Moore-Penrose pseudoinverse (Moore, 1920). Notably, the isotropic constraint on the uniquenesses provides the link from the factor analysis model to probabilistic principal component analysis (PPCA) (Tipping & Bishop, 1999).

The rotational invariance property which makes FA models non-identifiable is well known: most covariance matrices Σ cannot be uniquely factored as $\Lambda \Lambda^\top + \Psi$. As in McParland et al. (2014), this identifiability problem is addressed offline using the parameter expanded approach of Ghosh & Dunson (2008) and Procrustean methods.

2.2 Mixtures of Factor Analysers

A popular approach to model-based clustering in high-dimensional data settings is the mixture of factor analysers (MFA) model (Ghahramani & Hinton, 1996; McLachlan & Peel, 2000; McNicholas & Murphy, 2008). This finite mixture model allows each of G clusters to be modelled using a cluster-specific FA model. To facilitate estimation, a latent cluster indicator vector $\underline{z}_i = (z_{i1}, \dots, z_{iG})^\top$ is introduced such that

$$z_{ig} = \begin{cases} 1 & \text{if observation } i \in \text{cluster } g \\ 0 & \text{otherwise.} \end{cases}$$

Under the Bayesian paradigm, these latent cluster labels \underline{z}_i are assumed to follow a $\text{Mult}(1, \underline{\pi})$ distribution, where $\underline{\pi} = (\pi_1, \dots, \pi_G)^\top$ are the cluster mixing proportions, which sum to 1, and for which a symmetric uniform Dirichlet prior is assumed:

$$\underline{\pi} \sim \text{Dir}(\underline{\alpha} = \underline{1}) \quad (1)$$

It may be useful to constrain the mixing proportions to be equal across clusters in some settings. After marginalising out the latent cluster labels, MFA yields a parsimonious finite sum covariance structure for the observed data

$$f(\underline{x}_i) = \sum_{g=1}^G \pi_g \text{MVN}_p(\underline{\mu}_g, \Lambda_g \Lambda_g^\top + \Psi_g) \quad (2)$$

where $\underline{\mu}_g$, Λ_g , and Ψ_g denote the cluster-specific factor analysis parameters and for which inference is straightforward under a Gibbs sampling framework.

2.2.1 Limitations and Practical Issues

The main limitation of clustering via MFA, and the impetus underpinning IMIFA, is that values for G and q must be specified in advance of model fitting. Usually a range of MFA models are fitted for different values of G and q , and the pair of values optimising some model selection criterion is chosen. Notably, $q = 0$ is permitted. While it is possible to fit models where q differs across clusters, the model space becomes enormous and conducting an exhaustive search is computationally expensive. As a result, the fitting of MFA models in which the number of factors is cluster-specific is rarely considered.

In practice a number of model selection criteria are usually evaluated for the range of fitted MFA models, with different criteria often suggesting different optimal models. Thus the task of choosing the optimal MFA model becomes intertwined with choosing a suitable criterion, which can be contentious. This reliance on model selection tools makes selecting the optimal MFA model a fraught task. In what follows, optimal FA and MFA models are chosen using the BIC-MCMC criterion (Frühwirth-Schnatter, 2011):

$$\text{BIC-MCMC} = 2 \ln \tilde{\mathcal{L}} - \vartheta \ln N$$

where $\tilde{\mathcal{L}}$ denotes the largest log-likelihood value calculated for each retained posterior sample, and $\vartheta = G(pq - q(q-1)/2 + 2p) + G - 1$ is the effective number of parameters, assuming Ψ_g is unconstrained.

Another practical issue is the non-identifiability phenomenon of label switching (Frühwirth-Schnatter, 2010) which here is addressed offline using the cost-minimising permutation suggested by the square assignment algorithm (Carpaneto & Toth, 1980).

2.3 Mixtures of Infinite Factor Analysers

In MFA models q must be chosen in advance and is typically assumed to be the same across clusters. Here, to overcome these difficulties infinite factor analysis (IFA) models are employed, leading to the novel mixture of infinite factor analysers (MIFA). IFA models assume the multiplicative gamma process (MGP) shrinkage prior (Bhattacharya & Dunson, 2011) on the loadings matrix Λ . This prior allows the degree of shrinkage towards zero to increase as the column index $k \rightarrow \infty$. The prior is placed on the parameter expanded loadings matrix, which has no restrictions on its entries, thereby making the induced prior on the covariance matrix invariant to the ordering of the variables. The MGP prior is conjugate and thus the Gibbs sampler can be used, allowing block updating of the loadings matrix. In the MIFA context, the MGP prior is

$$\begin{aligned}\lambda_{jkg} &| \phi_{jkg}, \tau_{kg} \sim N(0, \phi_{jkg}^{-1} \tau_{kg}^{-1}) \\ \phi_{jkg} &\sim \text{Ga}(\nu, \varrho) \\ \tau_{kg} &= \prod_{h=1}^k \delta_{hg} \\ \delta_{1g} &\sim \text{Ga}(\alpha_1, \beta_1), \quad \delta_{hg} \sim \text{Ga}(\alpha_2, \beta_2) \quad \forall h \geq 2\end{aligned}\tag{3}$$

where τ_{kg} is a global shrinkage parameter for the k -th column in the loadings matrix of cluster g , for $k = 1, \dots, \infty$, and $\text{Ga}(\nu, \varrho)$ denotes the gamma distribution with mean ν/ϱ . The function of the local shrinkage parameters $\phi_{1kg}, \dots, \phi_{pkg}$ for the p elements in column k of the loadings matrix for cluster g is to induce sparsity. In practice, the number of effective factors can at most be equal to the number of variables p . A schematic illustration of the MGP prior is given in Figure 1.

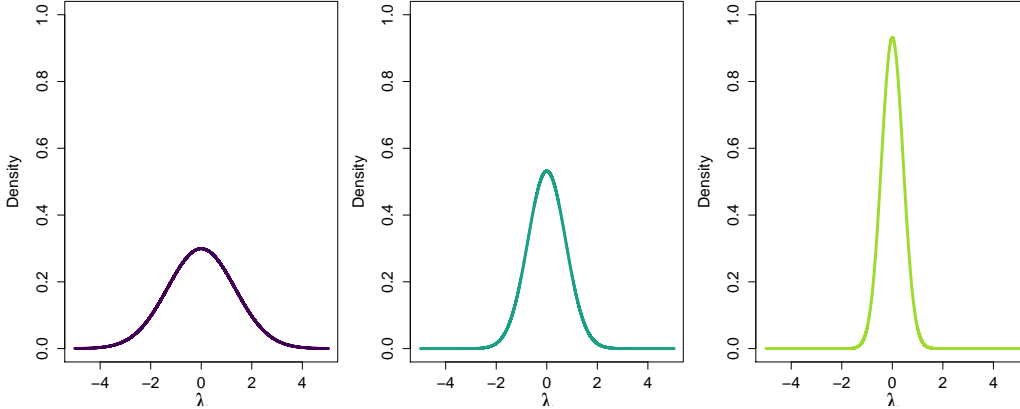


Figure 1: Density of the first, second, and third columns, respectively, of a typical cluster-specific loadings matrix under the MGP shrinkage prior.

Bhattacharya & Dunson (2011) fix $\beta_1 = \beta_2 = 1$, and recommend that $\alpha_2 > 1$. However, Durante (2017) shows that the MGP prior induces inverse gamma priors on the parameters $\tau_g^{-1} = \{\tau_{1g}^{-1}, \tau_{2g}^{-1}, \dots\}$. This implies that the column-specific variances only decrease in expectation as the column index k increases, such that the MGP prior assigns growing mass to small neighbourhoods of 0, under the restriction $\alpha_2 > \beta_2 + 1$. Durante (2017) also recommends that α_2 be moderately large relative to α_1 to ensure the cumulative shrinkage property, for which the prior was developed, holds.

Bhattacharya & Dunson (2011) also assume a $\text{Ga}(\nu, \nu)$ prior for the local shrinkage parameters, however the more general parameterisation in (3) is considered here, to facilitate control of the degree of non-informativeness of the prior. In the spirit of Durante (2017), such a specification induces local shrinkage *a priori* provided the expectation $\nu/(\nu-1)$ of the induced inverse-gamma prior on each ϕ_{jkg}^{-1} is ≤ 1 . It is generally advisable that local and global shrinkage hyperparameters are chosen such that the first two moments of the associated hyper-prior are defined. Although MGP hyperparameters remain fixed in what follows, they can be learned via the introduction of Metropolis-Hastings steps. In any case, when extending this prior to mixture models, α_1 and α_2 tend to need to be higher than the values suggested by Bhattacharya & Dunson (2011), in order to enforce a greater degree of shrinkage: there will be less data in each cluster from which the local and global shrinkage parameters can be learned under the MIFA model, compared to fitting the IFA model on the full data set.

2.3.1 The Adaptive Gibbs Sampler

In practical situations, relatively few important factors are expected compared to the number of variables p . When performing inference on MIFA models with the MGP prior, rather than fixing a large truncation level, an adaptive Gibbs sampler (AGS) is employed which adaptively shrinks and grows the loadings matrices to have finite numbers of columns, through selection of the number of ‘active’ factors. This practically facilitates posterior computation while closely approximating the infinite factor model, without requiring pre-specification of $\underline{Q} = (q_1, \dots, q_G)^\top$. However, a strategy is required for choosing appropriate truncation levels, \hat{q}_g , that strike a balance between missing important factors and wasting computational effort.

For computational reasons, a conservatively high upper bound is initially used, such that $\hat{q}_g = \min(\lfloor 3 \ln(p) \rfloor, p, N - 1) \forall g$. The number of factors in each Λ_g is then adaptively tuned as the MCMC chain progresses. Adaptation can be made to occur only after the burn-in period has elapsed, in order to ensure the true posterior distribution is being sampled from before truncating the loadings matrices. At the t -th iteration, adaptation occurs with probability $p(t) = \exp(-b_0 - b_1 t)$, with b_0 and b_1 chosen so that adaptation occurs often at the beginning of the chain but then decreases exponentially fast in frequency. Here $b_0 = 0.1$ and $b_1 = 5 \times 10^{-5}$ are used.

Practically, at iteration t , a uniform random number u_t between 0 and 1 is generated. If $u_t \leq p(t)$, columns in the loadings matrices having some pre-specified proportion of elements ς in a small neighbourhood ϵ of zero are monitored. Choice of ς and ϵ can be delicate issues: here $\varsigma = \lfloor 0.7 \times p \rfloor / p$ and $\epsilon = 0.1$ are found to strike an appropriate balance in most applications. If there are no such columns, an additional column is added by simulation from the MGP prior. Otherwise redundant columns are discarded, the AGS proceeds with fewer loadings columns, and all parameters corresponding to non-redundant columns are retained. As there is only one matrix η of latent factors, its dimensions at a given iteration are set to $p \times \tilde{q} = p \times \max(\underline{Q}(t))$. Rows of η corresponding to observations currently assigned to a cluster with fewer latent factors than \tilde{q} are padded out with zeros. Unlike the IFA model of Bhattacharya & Dunson (2011), and the parsimonious Gaussian mixture models of McNicholas & Murphy (2008), in MIFA \hat{q}_g is allowed to shrink to zero, thereby allowing a diagonal covariance structure within a cluster. If this occurs, the decision to simulate a new column is based on a binary trial with probability $1 - \varsigma$, as there are no loadings columns to monitor.

The number of active factors in each cluster is stored for each MCMC sample after burn-in and thinning. A bar chart approximation to the posterior distribution of q_g can be constructed; The posterior mode is used to estimate each q_g , with credible intervals quantifying uncertainty. Other details pertinent to the AGS, including full conditional distributions, are provided in Section 2.5.5 when the flagship IMIFA model is elaborated.

The main advantages of MIFA are that different clusters can be modelled by different numbers of factors and that the model search is significantly reduced to one for G only, as q_g is estimated automatically during model fitting. Here, for MIFA models, the optimal G is chosen via BICM (Raftery et al., 2007), with

$$\text{BICM} = 2 \ln \tilde{\mathcal{L}} - 2s_l^2 \ln N$$

where s_l^2 is the sample variance of the log-likelihood values calculated for each posterior sample after burn-in and thinning. This criterion is particularly useful in the context of nonparametric models where the number of free parameters is difficult to quantify.

The present work represents the first generalisation of the MGP prior and its associated AGS routine to the mixture context. Wang et al. (2016) develop a related model employing a multiplicative exponential process prior in the context of high-dimensional density estimation. Other nonparametric approaches to inferring the number of factors include Knowles & Ghahramani (2007) and Ročková & George (2016), in which an Indian Buffet Process (IBP) prior is assumed on an infinite binary matrix underlying the loadings matrix, thereby selecting features of interest, with weights on the selected loadings assumed to be Gaussian. However, such approaches assume a single sparse infinite factor model for the whole data set. Chen et al. (2010) consider the IBP approach in a mixture context, applied in a manifold learning setting. While such an approach may prove advantageous for clustering notably sparse data, MIFA’s elegant synoptic property that facilitates estimation and uncertainty quantification of the number of cluster-specific factors, in a parsimonious manner, is an advantageous feature.

2.4 Overfitted Mixtures of (Infinite) Factor Analysers

While MIFA obviates the need to pre-specify q , significantly easing the computational burden, the issue of model choice is not yet fully resolved. Overfitted mixtures (Rousseau & Mengersen, 2011; van Havre et al., 2015) are one means of extending MIFA to obviate the need to choose the optimal G . Indeed, Papastamoulis (2018) propose an overfitted mixture of finite factor analysers, though the method does not facilitate estimation or uncertainty quantification of the numbers of cluster-specific factors.

In overfitted mixtures, the prior on the mixing proportions (1) plays an important role. Estimation is approached by initially overfitting the number of clusters expected to be present, and specified conditions on the Dirichlet hyperparameter vector $\underline{\alpha}$ encourage the emptying out of excess components in the posterior distribution. Here, the overfitted mixture of factor analysers (OMFA) model and the overfitted mixture of infinite factor analysers (OMIFA) model are reviewed and introduced, respectively.

To initialise the overfitted models, a conservatively high number of clusters $G^* = \max(25, \lceil 3 \ln(N) \rceil)$ is chosen, and remains fixed throughout the MCMC chain. Typically G^* is much greater than the ‘true’ number of clusters. However when G^* is close to or exceeds N , it is preferable to initialise G^* closer to the expected truth ($\approx \ln(N)$), in order to ensure poorly populated clusters are not dominated by the priors. An exchangeable prior is assumed whereby each α_g is set to a common value, usually less

than $\mathcal{D}/2$ where \mathcal{D} is the number of per-cluster free parameters. This is small enough to favour emptying extra clusters *a priori* (Rousseau & Mengersen, 2011); the symmetric uniform prior in (1) is rather indifferent in this respect. For the implementations considered here, each α_g is fixed at a common value, much less than $\mathcal{D}/2$. Furthermore, by setting each $\alpha_g = \gamma/G^*$, the prior approximates a Dirichlet process with concentration parameter γ as G^* tends to infinity (Neal, 2000; Ishwaran et al., 2001). The number of non-empty clusters, G_0 , is recorded at each iteration of the MCMC chain as follows:

$$G_0 = G^* - \sum_{g=1}^{G^*} \mathbb{1} \left(\sum_i^N z_{ig} = 0 \right)$$

where $\mathbb{1}(\cdot)$ is the indicator function. The true G is estimated by the G_0 value visited most often by the sampler. Cluster-specific inference is conducted only on the samples corresponding to those visits.

Choosing α is a delicate issue, often making implementation of overfitted models challenging. If α is too large, few clusters will be emptied; if it is too small, the estimated number of clusters shrinks close to the true G , but mixing proportions become so small that new clusters are rarely formed as the sampler proceeds. An additional limitation is the difficulty in defining $\mathcal{D}/2$ for both finite factor and infinite factor overfitted models. Furthermore, the sampler must carry around and simulate the empty clusters from the priors, bringing computational overhead. For the OMIFA model, the AGS is modified to handle empty clusters about which there is no information: these empty clusters are restricted to having \tilde{q} factors, i.e. the same number of columns currently in the matrix of factor scores, η , either by truncation or by padding with zeros, as appropriate.

2.5 Infinite Mixtures of (Infinite) Factor Analysers

An alternative means of extending MFA and MIFA to automate estimation of G is provided by considering infinite mixture models. Such consideration leads, respectively, to the infinite mixture of factor analysers (IMFA) model and the flagship infinite mixture of infinite factor analysers (IMIFA) model, thus completing the hierarchy of the IMIFA family of models. IMFA and IMIFA are nonparametric mixture models which employ a two-parameter Poisson-Dirichlet process (also known as a Pitman-Yor process (Pitman & Yor, 1997)) as a prior; the well-known Dirichlet process is a special case and is thus used as the starting point in the development of the IMFA and IMIFA models below.

2.5.1 Dirichlet Process Mixture Models

Dirichlet processes (DP) (Ferguson, 1973) are stochastic processes whose draws are random probability measures: $H \sim \text{DP}(\alpha, H_0)$ denotes a DP probability distribution H , with base distribution H_0 and concentration parameter α . The base distribution H_0 can be interpreted as the mean of the DP, while α expresses the strength of belief in H_0 . Though the DP is the cornerstone of Bayesian nonparametric inference, the DP prior is often employed in semiparametric hierarchical modelling. This approach is known as the Dirichlet Process Mixture Model (DPMM) (Antoniak, 1974):

$$\begin{aligned} \underline{x}_i | z_{ig} = 1, \theta_g &\sim f(\underline{x}_i; \theta_g) \\ \theta_g &\sim H \\ H &\sim \text{DP}(\alpha, H_0) \end{aligned}$$

For IMFA and IMIFA, H_0 comes from the factor-analytic mixture (2), such that

$$f(\underline{x}_i) = \sum_{g=1}^{\infty} \pi_g \text{MVN}_p \left(\underline{\mu}_g, \Lambda_g \Lambda_g^\top + \Psi_g \right) \quad (4)$$

In the IMFA model, each Λ_g has a finite number of columns. For IMIFA, Λ_g theoretically has infinitely many columns, $\forall g$. Conjugate prior distributions, with additional layers for hyperparameters, are as specified previously for the related MFA and MIFA models.

There exist several equivalent metaphors which motivate methods of yielding samples from a DP without representing the infinite dimensional variable G explicitly. These include the Chinese restaurant process (Aldous, 1985), the Pólya urn scheme (Blackwell & MacQueen, 1973), and the stick-breaking representation (Sethuraman, 1994). The novel IMFA and IMIFA models proposed here focus on the latter. Furthermore, MCMC sampling strategies for DPMMs can be divided into two families: marginal methods, which integrate out the infinite dimensional probability measure H and represent the partition structure of the data directly (Escobar, 1994; Escobar & West, 1995; Neal, 2000), and conditional methods, which sample a sufficient but finite number of clusters at each iteration. Conditional methods include retrospective sampling (Papaspiliopoulos & Roberts, 2008), truncation (Ishwaran et al., 2001), and slice sampling (Walker, 2007; Kalli et al., 2011), the latter of which is adopted here. In practice, the number of non-empty clusters can be at most equal to N , even if theoretically G is infinite, as illustrated in Figure 2a. Notably, the growth rate of $\mathbb{E}(G)$ is known to be logarithmic in N (Antoniak, 1974). Thus the same G^* value detailed in Section 2.4 for the overfitted OMFA and OMIFA models is adopted here to initialise the IMFA and IMIFA samplers, with similar caution advised for data sets with a small sample size.

2.5.2 The Stick-Breaking Representation

An elegant constructive characterisation of the DP is given by the stick-breaking representation (Sethuraman, 1994). The IMFA and IMIFA models use this as a prior process for generating the mixing proportions of the infinite mixture distribution in (4). This representation metaphorically views $\{\pi_1, \pi_2, \dots\}$ as pieces of a unit-length stick that is sequentially broken in an infinite process, with stick-breaking proportions $\underline{v} = \{v_1, v_2, \dots\}$, according to independent realisations of a Beta distribution. This stick-breaking representation can be summarised as follows

$$\begin{aligned} v_g &\sim \text{Beta}(1, \alpha) & \theta_g &\sim H_0 \\ \pi_g &= v_g \prod_{l=1}^{g-1} (1 - v_l) & H &= \sum_{g=1}^{\infty} \pi_g \delta_{\theta_g} \sim \text{DP}(\alpha, H_0) \end{aligned} \quad (5)$$

where δ_θ is the Dirac delta centered at θ , such that draws are composed of a sum of infinitely many point masses, and $\theta_g = \{\underline{\mu}_g, \Lambda_g, \Psi_g\}$ denotes the cluster-specific set of parameters of the FA or IFA models.

2.5.3 Slice Sampling Infinite Mixture Models

In order to deal with the problematic issue of handling countably infinite numbers of values in a DPMM, a slice sampler is employed to make finite the number of objects to be sampled within each iteration of a Gibbs sampler. For each observation i , an

auxiliary variable $u_i > 0$ is introduced, which preserves the marginal distribution of the data \underline{x}_i and facilitates writing the conditional density of $\underline{x}_i | u_i$ as a finite mixture model. As such, u_i has the effect of adaptively truncating the number of components needed to be sampled. Denoting by $\underline{\xi} = \{\xi_1, \xi_2, \dots\}$ a decreasing sequence of infinite quantities which sum to 1, the joint distribution of (\underline{x}_i, u_i) is given by

$$f(\underline{x}_i, u_i | \theta, \underline{\xi}) = \sum_{g=1}^{\infty} \pi_g \text{Unif}(u_i; 0, \xi_g) f(\underline{x}_i; \theta_g)$$

with
$$f(\underline{x}_i; \theta) = \sum_{g=1}^{\infty} \pi_g f(\underline{x}_i; \theta_g)$$

and
$$f(u_i; \underline{\xi}) = \sum_{g=1}^{\infty} \pi_g \text{Unif}(u_i; 0, \xi_g) = \sum_{g=1}^{\infty} \frac{\pi_g}{\xi_g} \mathbb{1}(u_i < \xi_g)$$

Since only a finite number of ξ_g are greater than u_i , by denoting $\mathcal{A}_{\xi}(u_i) = \{g : u_i < \xi_g\}$, the conditional density of $\underline{x}_i | u_i$ can be written as a *finite* mixture model, meaning the infinite mixture of factor analysers model (4) can now be sampled from:

$$f(\underline{x}_i | u_i, \theta) = \frac{f(\underline{x}_i, u_i; \theta, \underline{\xi})}{f(u_i; \underline{\xi})} = \sum_{g \in \mathcal{A}_{\xi}(u_i)} \frac{\pi_g}{\xi_g f(u_i; \underline{\xi})} f(\underline{x}_i; \theta_g)$$

Typical implementations of the slice sampler arise when $\xi_g = \pi_g$ (Walker, 2007) but ‘independent’ slice-efficient sampling (Kalli et al., 2011) allows for a deterministic decreasing sequence, e.g. geometric decay, given by $\xi_g = (1 - \rho)\rho^{g-1}$ where $\rho \in (0, 1]$ is a fixed value. The value of ρ must be chosen with care: high values generally lead to better mixing but longer run times, as the cardinality of $\mathcal{A}_{\xi}(u_i)$ increases, and *vice versa*. Setting $\rho = 0.75$ appears to strike an appropriate balance in the IMFA and IMIFA applications considered here; $\rho = 0.5$ is also interesting, guaranteeing $\xi_g = \mathbb{E}(\pi_g)$. With the stick-breaking prior and independent slice-efficient sampler, mixture components and their corresponding parameters are reordered at each iteration such that the mixing proportions form a decreasing sequence, as the stick-breaking prior is not invariant to the order of cluster labels (Papaspiliopoulos & Roberts, 2008; Hastie et al., 2014).

2.5.4 Extension to Pitman-Yor Processes

The two-parameter Poisson-Dirichlet process is a popular generalisation of the DP (Perman et al., 1992; Pitman & Yor, 1997), frequently referred to as the Pitman-Yor process (henceforth PYP). The PYP (α, d, H_0) prior introduces a discount parameter $d \in [0, 1)$, with the constraint $\alpha > -d$. Conveniently, the PYP prior has its own stick-breaking construction, compatible with the slice sampler, where $v_g \sim \text{Beta}(1 - d, \alpha + gd)$, meaning inference for IMFA and IMIFA under the PYP prior can be easily implemented in the MCMC sampling framework. While the PYP prior reduces to the DP prior when $d = 0$, some important distributional features fundamentally differ when $d \neq 0$ (Figure 2b). The PYP prior exhibits heavier tail behaviour, and allows the stick-breaking distribution to vary according to the cluster index, without sacrificing much in the way of tractability. In particular, non-zero d values have the effect of flattening the DP prior, implying flexibility to more correctly uncover the true number of clusters and ability to control the degree of non-informativeness of the prior. Under the PYP prior, the growth rate of $\mathbb{E}(G)$ is Zipfian rather than logarithmic in N .

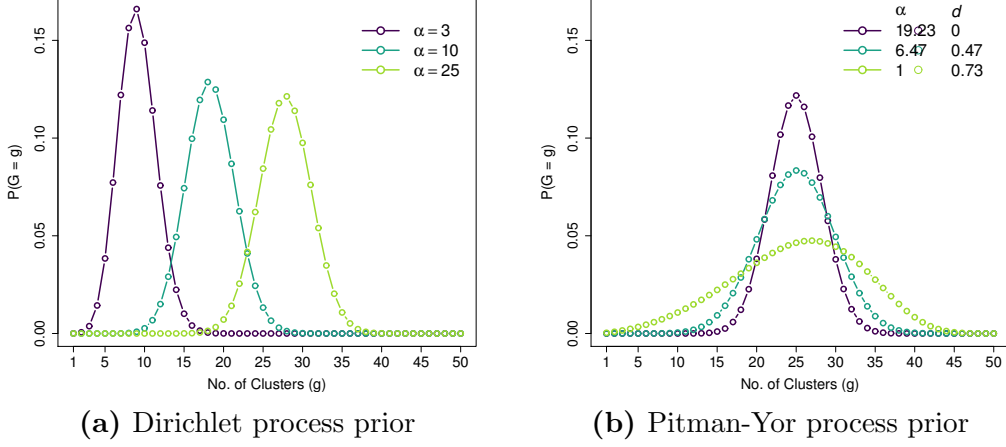


Figure 2: DP and PYP priors when $N = 50$, with different concentration and discount parameter settings. Under the DP prior, mass shifts to the right with increasing dispersion as α increases. Under the PYP prior, with parameters fixed to ensure $\mathbb{E}(G_{50}) = 25$, a heavier-tailed, less informative prior is obtained as d increases.

2.5.5 Inference for Infinite Mixtures of Factor Analysers Models

For clarity, what follows focuses on IMIFA with a PYP prior where inference proceeds via the independent slice-efficient sampler with geometric decay. Inference assuming the DP prior is closely related, as is inference for other models in the IMIFA family. The MGP prior is assumed for infinite factor models (IMIFA, OMIFA, MIFA, IFA) with the loadings prior in finite factor models (IMFA, OMFA, MFA, FA) as given in Section 2.1.1. The joint distribution of the IMIFA model is proportional to:

$$\begin{aligned}
f(X, \eta, Z, \underline{u}, \underline{\Upsilon}, \theta) &\propto f(X | \eta, Z, \underline{u}, \underline{\Upsilon}, \theta) f(\eta | \underline{u}) f(Z, \underline{u} | \underline{\Upsilon}, \pi) f(\underline{\Upsilon} | \alpha, d) f(\theta) \\
&= \left\{ \prod_{i=1}^N \prod_{g \in \mathcal{A}_{\xi}(u_i)} \text{MVN}_p(\underline{x}_i; \underline{\mu}_g + \Lambda_g \underline{\eta}_i, \Psi_g)^{z_{ig}} \right\} \\
&\quad \left\{ \prod_{i=1}^N \prod_{g \in \mathcal{A}_{\xi}(u_i)} \text{MVN}_q(\underline{\eta}_i; 0, \mathcal{I}_q) \right\} \\
&\quad \left\{ \prod_{i=1}^N \prod_{g=1}^{\infty} \left(\frac{\pi_g}{\xi_g} \mathbb{1}(u_i < \xi_g) \right)^{z_{ig}} \right\} \left\{ \prod_{g=1}^{\infty} \frac{(1 - v_g)^{\alpha + gd - 1}}{v_g^d \text{B}(1 - d, \alpha + gd)} \right\} f(\theta)
\end{aligned}$$

where $\text{B}(\cdot)$ is the Beta function and $f(\theta)$ is the product of the collection of relevant conjugate priors defined previously. Only the parameters of the ‘active’ clusters for which $g \in \mathcal{A}_{\xi}(u_i)$ are sampled at each iteration; the number of active clusters is given by $\tilde{G} = \max_{1 \leq i \leq N} |\mathcal{A}_{\xi}(u_i)|$ where $|\cdot|$ denotes cardinality. This integer varies across iterations, but stays fixed at each iteration, even if theoretically infinite, and can even take the value 1. However, \tilde{G} is only regarded as a set of proposals as to where to allocate observations; it is the non-empty subset of clusters that is of inferential interest. The algorithm is initialised with a conservatively high value for the number of clusters, above the anticipated number to which the algorithm will converge, in the spirit of [Hastie et al. \(2014\)](#). The true G is estimated by the G_0 value visited most often, with cluster-specific inference conducted only on samples corresponding to those visits.

As all posterior conditional distributions have standard form, the adaptive inferential algorithm for IMIFA proceeds via efficient Gibbs updates. The value of q_g at a given iteration is denoted \tilde{q}_g and \tilde{G} is the current number of active clusters. The number of observations within a given cluster is n_g , with $\underline{n} = \{n_1, \dots, n_{\tilde{G}}\}$ s.t. $N = \sum_{g=1}^{\tilde{G}} n_g$. It is well known that Bayesian approaches to clustering can be sensitive to the initialisation of the cluster allocations. While starting values for \underline{z}_i , and by extension \underline{n} , can be obtained by any means, here they are obtained via the popular R package **mclust** (Fraley & Raftery, 2002; Scrucca et al., 2016), unless otherwise stated. Other parameter starting values are simulated from the appropriate prior distribution. While the parameter specifications of the posterior conditional distributions are deferred to Appendix A for clarity, the Gibbs steps for IMIFA are as follows, for $g = 1, \dots, \tilde{G}$:

$$\begin{aligned}
\underline{\mu}_g \mid \dots &\sim \text{MVN}_p \\
\underline{\eta}_{i:z_{ig}=1} \mid \dots &\sim \text{MVN}_{\tilde{q}_g} \quad \text{for } i = 1, \dots, n_g \\
\underline{\Lambda}_{jg} \mid \dots &\sim \text{MVN}_{\tilde{q}_g} \quad \text{for } j = 1, \dots, p \\
\psi_{jg} \mid \dots &\sim \text{IG} \quad \text{for } j = 1, \dots, p \\
\phi_{jkg} \mid \dots &\sim \text{Ga} \quad \text{for } j = 1, \dots, p \text{ and } k = 1, \dots, \tilde{q}_g \\
\delta_{1g} \mid \dots &\sim \text{Ga} \\
\delta_{kg} \mid \dots &\sim \text{Ga} \quad \text{for } k = 2, \dots, \tilde{q}_g \\
v_g \mid \dots &\sim \text{Beta} \\
u_i \mid \dots &\sim \text{Unif} \quad \text{for } i = 1, \dots, N
\end{aligned}$$

In the context of the IMIFA and IMFA models:

$$z_{ig} = 1 \mid \dots \propto f\left(\underline{x}_i \mid \underline{\mu}_g, \Lambda_g \Lambda_g^\top + \Psi_g\right) \frac{\pi_g}{\xi_g} \mathbb{1}(u_i < \xi_g)$$

whereas under the finite and overfitted mixtures (i.e. MFA, MIFA, OMFA, and OMIFA):

$$\underline{z}_i \mid \underline{x}_i, \dots \sim \text{Mult}$$

In both cases, sampling is performed efficiently, in a numerically stable fashion, using the unnormalised log-probabilities, with the aid of the Gumbel-Max trick (Yellott, 1977). Furthermore, as several of the posterior conditional distributions are multivariate Gaussian, utilising the Cholesky decomposition of covariance matrices and employment of block updates significantly speeds up the algorithm (Rue & Held, 2005).

Sampling the parameters of the PYP requires Metropolis-Hastings steps. A hyper-prior $\alpha \mid d \sim \text{Ga}(\alpha + d \mid a, b)$ is given to the concentration parameter α conditional on d , which includes the constraint $\alpha > -d$ by shifting the support of the gamma density to $(-d, \infty)$. The hyper-prior assumed for the discount parameter d is a mixture of a point-mass at zero and a continuous beta distribution, in order to consider the DP special case where $d = 0$ with positive probability, i.e. $d \sim \kappa \delta_0 + (1 - \kappa) \text{Beta}(d \mid a', b')$ (Carmona et al., 2018). Of the sampled d values, the estimated proportion of which are 0, $\hat{\kappa}$, can be used to assess whether the data arose from a DP or PYP at little extra computational cost. Should a DP prior be specifically desired, $\text{Ga}(a, b)$ hyper-prior for α is assumed here, which is learned through the auxiliary variable routine of West (1992) via Gibbs updates from a weighted mixture of two gamma distributions, although it remains fixed in many applications (e.g. Ishwaran et al. (2001)).

Finally, as state spaces for applications of IMIFA to real data can be highly multi-modal with well separated regions of high posterior probability coexisting, corresponding to clusterings with different numbers of components, the label switching moves below (Papaspiliopoulos & Roberts, 2008) are incorporated in order to improve mixing:

1. Swap labels of two randomly chosen non-empty clusters g and h with probability $p_1 = \min \left\{ 1, (\pi_h/\pi_g)^{n_g - n_h} \right\}$.
2. Swap labels of neighbouring active clusters g and $g + 1$ with probability $p_2 = \min \left\{ 1, (1 - v_{g+1})^{n_g} / (1 - v_g)^{n_{g+1}} \right\}$ and, if accepted, also swap v_g and v_{g+1} .

These are complimentary moves which are effective at swapping similar and unequal clusters, respectively. Parameters are reordered accordingly after each accepted move.

2.5.6 Assessing Model Fit

As is good statistical practice, posterior predictive model checking (Gelman et al., 2003) is employed to assess model fit. Sampled values of the model parameters from the MCMC chain are used to generate replicate data. Given the multivariate nature of the data, measures of discrepancy between the sample covariance \mathbf{S} and the estimated covariance Σ^r of replicate data set r are used to study model adequacy (Ansari et al., 2002; Nyamundanda et al., 2014). For a G component Gaussian mixture model, the jk^{th} term in the overall covariance matrix, Σ , can be obtained as

$$\Sigma_{j,k} = \sum_{g=1}^G \pi_g \Sigma_{j,k}^{(g)} + \sum_{g=1}^G \pi_g \mu_j^{(g)} \mu_k^{(g)} - \left(\sum_{g=1}^G \pi_g \mu_j^{(g)} \right) \left(\sum_{g=1}^G \pi_g \mu_k^{(g)} \right)$$

where $\Sigma^{(g)}$ denotes the covariance of cluster g , parameterised by $\Lambda_g \Lambda_g^\top + \Psi_g$ under the factor-analytic framework, and $\mu_j^{(g)}$ denotes the mean of variable j in cluster g . For infinite and overfitted models in the IMIFA family it is necessary to renormalise the mixing proportions after conditioning on the modal estimate of G . Thus, the estimated covariance matrix Σ^r can be computed for every valid sample and compared to \mathbf{S} using familiar metrics such as mean squared error (MSE) and root mean squared error (RMSE); the uncertainty in these metrics can also be quantified. Valid samples are those, after accounting for burn-in and thinning, where all G clusters have q_g or more columns in their loadings matrices. Normalising the RMSE value by the range of \mathbf{S} yields a further useful metric, NRMSE, which can be interpreted as a proportion.

3 Illustrative Applications

The flexibility and performance of IMIFA and its related models are demonstrated through applications to simulated data (Section 3.1), to benchmark Italian olive oil data (Section 3.2), to spectral metabolomic data from an epilepsy study (Section 3.3), and to handwritten digit data in the context of manifold learning (Section 3.4). Further results, visualisations thereof, and hyperparameter settings are included in the Appendices; in particular, an additional simulation study assessing the robustness of IMIFA is provided. All results are obtained through the associated R package **IMIFA** (Murphy et al., 2017); code to reproduce many of the results below is available in the **IMIFA** package vignette¹.

¹<https://cran.r-project.org/web/packages/IMIFA/vignettes/IMIFA.html>

The MCMC chains were run for 50,000 iterations, with the exceptions of Sections 3.1 and 3.4 in which 25,000 and 5,000 were run, respectively. In all cases, every 2nd sample was thinned and the first 20% of iterations were discarded as burn-in. Mixing and convergence were assessed visually (see Appendix C). All computations were performed on a Dell Inspiron 15 7000 series computer, equipped with a 3.50 GHz Intel Core i7-6700HQ processor and 16 GB of RAM. Where necessary, the optimal model is chosen by the BICM criterion, except for the FA and MFA models where the BIC-MCMC is used. Unless otherwise stated, data were mean-centered and unit scaled prior to analysis and the PYP prior was assumed for the infinite mixture models. Throughout, $\hat{\cdot}$ denotes the posterior mode, posterior mean, or optimal value, as relevant to the quantity of interest.

3.1 Simulation Study

The performance of the novel IMIFA model, in terms of estimation of both the number of clusters and the cluster-specific number of factors, is assessed through a thorough simulation study. Data with $G = 3$ clusters and $p = 50$ variables are simulated with $q_g = 4 \forall g$, and with $\underline{\pi} = \{1/3, 1/3, 1/3\}$ so that clusters are roughly equally sized. Model parameters are simulated, with $\underline{\eta}_i \sim \text{MVN}_q(\underline{0}, \underline{\mathcal{I}}_q)$, $\Lambda_{jg} \sim \text{MVN}_q(\underline{0}, \underline{\mathcal{I}}_q)$ and $\Psi_{jg} \sim \text{IG}(2, 1)$. To ensure clusters are reasonably closely located, $\underline{\mu}_g \sim \text{MVN}_p(-1 + 1(g-1), 1)$. The data are then simulated according to the conditional mixture model:

$$\underline{x}_i | \underline{\eta}_i \sim \sum_{g=1}^G \pi_g \text{MVN}_p(\underline{\mu}_g + \Lambda_g \underline{\eta}_i, \Psi_g)$$

Table 1: Aggregated simulation study results for the IMIFA model under different dimensionality scenarios and different settings of the concentration and discount parameters α and d (posterior mean estimates thereof in parentheses where appropriate). The modal estimates of G and associated estimates of $q_g \forall g$ are reported (with 95% credible intervals in brackets). Average run times are given and clustering performance is assessed through the average percentage error rate against the known cluster labels.

Dimension	α	d	G	q_1	q_2	q_3	Time (s)	Error (%)
N = 25 (N \ll p)	0.5	0	3 [3,3]	4 [2,7]	4 [2,7]	4 [2,7]	326	2.8
	1	0	3 [3,3]	4 [2,7]	4 [2,7]	4 [2,7]	328	0
	5	0	3 [3,4]	4 [2,7]	4 [2,7]	4 [2,7]	330	6.4
	Learned (1.09)	0	3 [3,3]	4 [2,7]	4 [2,7]	4 [2,7]	329	0
	Learned (1.07)	Learned (0.03)	3 [3,3]	4 [2,7]	4 [2,7]	4 [2,7]	334	0
N = 50 (N = p)	0.5	0	3 [3,3]	4 [3,6]	4 [3,6]	4 [3,6]	359	0
	1	0	3 [3,3]	4 [3,6]	4 [3,6]	4 [3,6]	367	0
	5	0	3 [3,3]	4 [3,6]	4 [3,6]	4 [3,6]	374	0
	Learned (0.90)	0	3 [3,3]	4 [3,6]	4 [3,6]	4 [3,6]	364	0
	Learned (0.88)	Learned (0.02)	3 [3,3]	4 [3,6]	4 [3,6]	4 [3,6]	373	0
N = 300 (N \gg p)	0.5	0	3 [3,3]	5 [4,6]	5 [4,6]	5 [4,6]	557	0
	1	0	3 [3,3]	5 [4,6]	5 [4,6]	5 [4,6]	563	0
	5	0	3 [3,3]	5 [4,6]	5 [4,6]	5 [4,6]	567	0
	Learned (0.62)	0	3 [3,3]	5 [4,6]	5 [4,6]	5 [4,6]	562	0
	Learned (0.61)	Learned (0.01)	3 [3,3]	5 [4,6]	5 [4,6]	5 [4,6]	570	0

To evaluate performance in different settings, sample sizes less than, equal to, and greater than p are considered, i.e. $N = 25, 50$, and 300. Sensitivity to DP and PYP parameters is explored by firstly assuming the DP prior with various values of α less than,

equal to, and greater than 1, and by allowing α to be learned as per West (1992), and secondly by incorporating Metropolis-Hastings steps to learn both α and d , assuming a PYP prior. Results, provided in Table 1, are based on ten replicate data sets.

Table 1 clearly demonstrates the IMIFA model’s excellent performance. The modal estimate of G is equal to the truth in all cases, with only the $N \ll p$, $\alpha = 5$ scenario showing some deviation in the 95% credible interval. Furthermore, in every case the true value of q_g is within the limits of the associated intervals which intuitively become narrower as more data accumulates. Finally, run times are very acceptable and clustering performance is mostly perfect. Overall, the IMIFA model exhibits capability to uncover structure within the simulated data sets, regardless of dimensionality.

3.2 The Benchmark Italian Olive Oil Dataset

Assessment of the performance of the IMIFA family of models is explored through application to the benchmark Italian olive oil data set (Forina et al., 1983) which is typically clustered using factor-analytic models (e.g. McNicholas (2010)). The data detail the percentage composition of 8 fatty acids in 572 Italian olive oils, known to originate from three areas: southern Italy, Sardinia and northern Italy. Within each area there are a number of different regions: southern Italy comprises north Apulia, Calabria, south Apulia, and Sicily, Sardinia is divided into inland Sardinia and coastal Sardinia, and northern Italy comprises Umbria, east Liguria, and west Liguria. As such the true number of clusters is hypothesised to correspond to either 3 areas or 9 regions.

The full family of IMIFA related models are fitted to the Italian olive oil data – from the basic FA model through to the flagship IMIFA model. Results are detailed in Table 2. Results for models which rely on pre-specification of G and/or q are based on considering $G = 1, \dots, 9$ and $q = 0, \dots, 6$. Clustering performance is evaluated using the adjusted Rand index (Hubert & Arabie, 1985) and percentage misclassification error rate, compared to the known 3-cluster area labels. The α parameter is reported as its fixed value or posterior mean, as appropriate.

Table 2: Results of applying the IMIFA family of models to the Italian olive oil data set, detailing the number of candidate models explored, total run time in seconds, run time taken relative to the IMIFA run, the fixed or posterior mean of α , the posterior mean of d , modal estimates of G and Q , and the adjusted Rand Index and error rate, as evaluated against the known area labels, under the optimal or modal model as appropriate.

Model	# Models	Time (s)	Rel. Time	α	d	G	Q	Adj. Rand	Error (%)
IMIFA	1	782	1.00	0.75	0.01	4	6, 2, 3, 2	0.93	8.57
IMFA	7	3661	4.68	0.88	0.01	5	6, 6, 6, 6, 6	0.92	10.31
OMIFA	1	818	1.05	0.02	–	5	6, 2, 2, 2, 2	0.90	15.56
OMFA	7	3336	4.27	0.02	–	5	6, 6, 6, 6, 6	0.85	15.91
MIFA	9	2608	3.33	1	–	5	5, 2, 2, 3, 2	0.91	14.86
MFA	63	11083	14.17	1	–	2	5, 5	0.82	17.13
IFA	1	78	0.10	–	–	1	6	–	–
FA	7	287	0.37	–	–	1	6	–	–

Table 2 clearly demonstrates the flexibility and accuracy of the developed family of models, and of the IMIFA model in particular which has the best clustering performance.

Additionally, IMIFA is the most computationally efficient model considered as it requires only one run and does not require any model selection criteria. This speed improvement would be exacerbated with larger data sets. The flexibility to model clusters using different numbers of factors, and the versatility afforded by the PYP prior, greatly improves clustering performance.

Figure 3 shows a barchart approximation to the posterior distribution of G , using the number of non-empty clusters stored at each iteration. The modal value of 4 is used as the estimate of the true number of clusters (with 95% credible interval: $G \in [4, 6]$), with the sampler visiting the 4-cluster solution in 72% of iterations not discarded due to burn-in and thinning. Under the modal IMIFA model, 323 of the 572 olive oils originate in southern Italy: this large cluster requires the largest number of factors (6 [3, 6]); the other clusters have notably smaller numbers (2 [1, 4], 3 [2, 5], and 2 [1, 3], with 95% credible intervals given in brackets).

Table 3a cross tabulates the MAP clustering against the 3 area labels and suggests the modal $\hat{G} = 4$ IMIFA solution makes geographic sense, in that the northern olive oils are split into two sub-clusters. Table 3b reports the confusion matrix in which olive oils from northern Italy are labelled by their associated region, yielding an adjusted Rand index of 0.996 and an error rate of just 0.7%. The other IMIFA related models also yielded improved adjusted Rand indices and error rates with this labelling. Details on the uncertainty in the cluster allocations is provided in Appendix C.

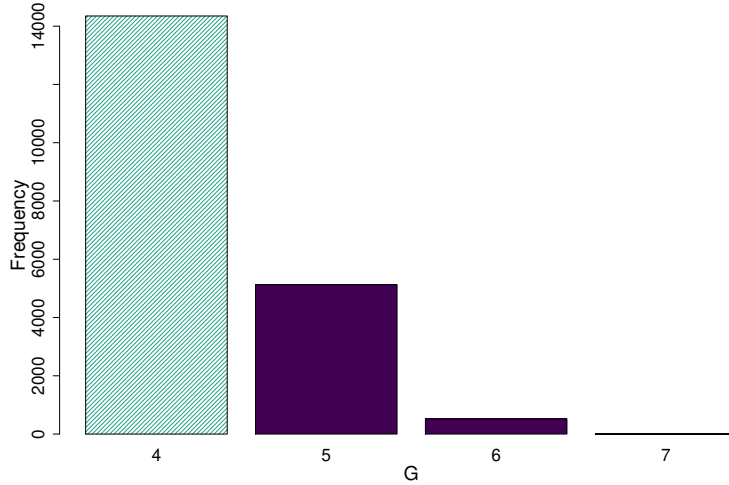


Figure 3: Posterior distribution of G uncovered by fitting the IMIFA model to the olive oil data set. The number of clusters is estimated by the modal value, $\hat{G} = 4$.

Table 3: Confusion matrices of the MAP IMIFA clustering of the Italian olive oils against (a) the known 3 area labels and (b) the new relabelling in which northern Italy is split into its constituent regions.

(a) 3 area cross tabulation					(b) 4 area cross tabulation				
	1	2	3	4		1	2	3	4
Southern Italy	323	0	0	0	Southern Italy	323	0	0	0
Sardinia	0	97	1	0	Sardinia	0	97	1	0
Northern Italy	0	0	103	48	Liguria	0	0	100	0
					Umbria	0	0	3	48

To assess sensitivity to starting values, the optimal IMIFA model was fit again, using both the k -means algorithm and model-based agglomerative hierarchical clustering (Scrucca et al., 2016) to initiate the cluster allocations. These runs led to similar inference about G and Q , and equivalent clustering performance.

Notably, IMIFA’s performance compares favourably to the unconstrained finite mixture of factor analysers model (McNicholas & Murphy, 2008), obtained using the **pgmm** R package: there the optimal model (fitted using maximum likelihood and chosen by BIC) has $\hat{G} = \hat{q} = 5$ with adjusted Rand index of 0.56 and error rate of 33.56%. Furthermore, IMIFA also outperforms **mclust**’s best unconstrained Gaussian finite mixture model, which yields an adjusted Rand index of 0.81 and an error rate of 26.05%. Note that while all IMIFA related models have been fitted to the standardised data, the optimal models achieved by **pgmm** and **mclust** were obtained on unscaled data.

It is also notable that within the set of IMIFA related models that rely on information criteria, those deemed optimal were not necessarily always optimal in a clustering sense. For instance, the candidate MIFA model with $\hat{G} = 4$ yields an adjusted Rand index of 0.94 and an error rate of 6.99%, with respect to the 3-group area labels, despite having a sub-optimal BICM. Lastly, for the IMIFA run, the proportion of zeros among sampled d values, $\hat{\kappa} \approx 0.92$, suggests similar inference would have resulted under a DP prior.

3.3 High-Dimensional Spectral Metabolomic Data

The performance of IMIFA in the context of high-dimensional data is demonstrated through application to real spectral metabolomic data for which $N \ll p$ (Figure 4). The data are nuclear magnetic resonance spectra consisting of $p = 189$ spectral peaks from urine samples of $N = 18$ participants, half of which are known to have epilepsy (Carmody & Brennan, 2010; Nyamundanda et al., 2010). Interest lies in whether the underlying clustering structure can be uncovered given the high-dimensional setting. Given that $N \ll p$, uniquenesses are constrained to be isotropic and as such the IMIFA model corresponds to an infinite mixture and infinite factor extension of PPCA. Results from fitting a number of the IMIFA family of models to these data are considered. Data were mean-centered and Pareto scaled prior to analysis (van den Berg et al., 2006).

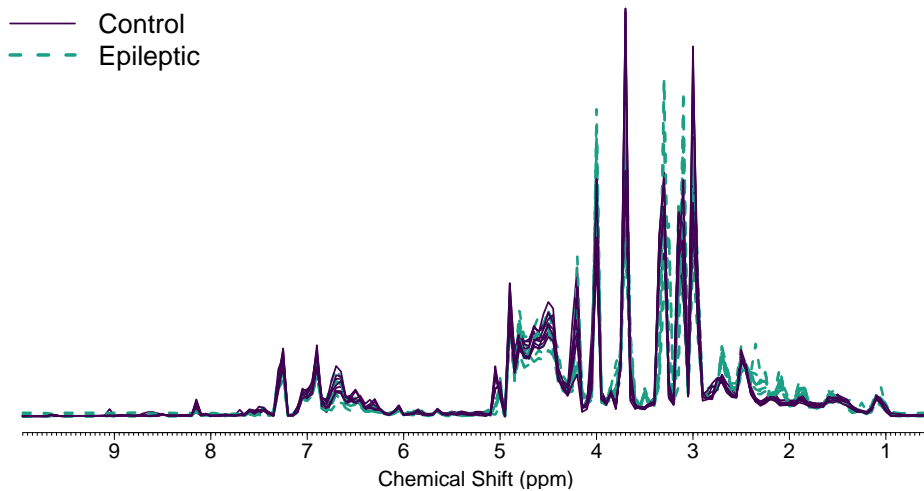


Figure 4: Spectral metabolomic data consisting of 18 spectral profiles of 9 healthy and 9 diseased study participants over $p = 189$ spectral bin regions.

When fitting MFA with $G = 2$ and $q = 0, \dots, 10$, the BIC-MCMC suggests $\hat{q} = 3$ and 2 participants are misclassified. Fitting MIFA for $G = 1, \dots, 5$, the BICM correctly chooses $\hat{G} = 2$ as optimal, and only one participant is clustered incorrectly. The modal estimates of the number of factors in each MIFA cluster are $\hat{q}_1 = 2$ and $\hat{q}_2 = 3$, with 95% credible intervals $q_1 \in [1, 4]$ and $q_2 \in [2, 5]$ (see Figure 5). Cluster 1 corresponds to the control group and Cluster 2 to the epileptic participants; the requirement for a more complex model with more factors for the epileptic participants is noteworthy. Furthermore, Figure 6 illustrates the $p \times \hat{q}_g$ posterior mean loadings matrices under the optimal MIFA model (based on the subset of retained samples with \hat{q}_g or more factors, after Procrustes rotation) showing the sparsity and shrinkage induced by the MGP prior and the notably greater complexity in the cluster relating to the epileptic participants.

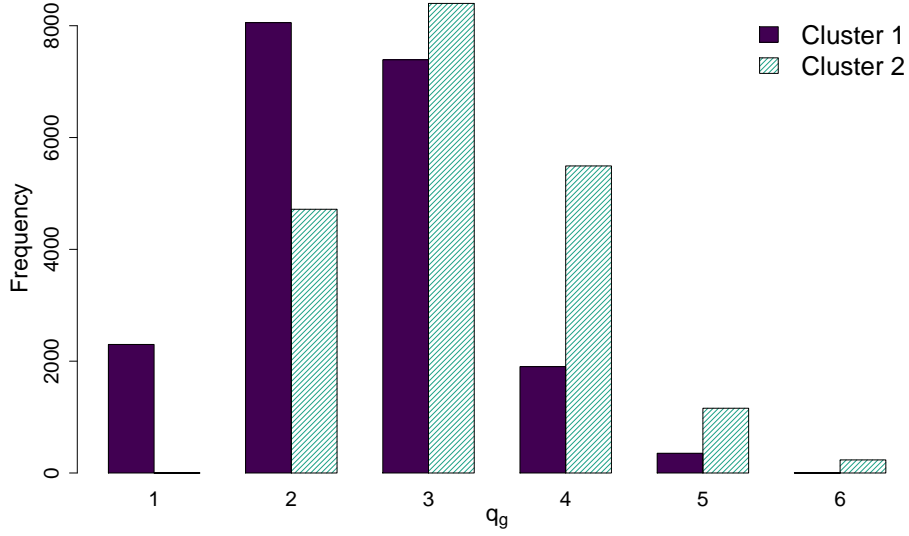


Figure 5: Posterior distribution of q_g uncovered by fitting MIFA to the metabolomic data. More factors are required for Cluster 2, encapsulating the epileptic participants.

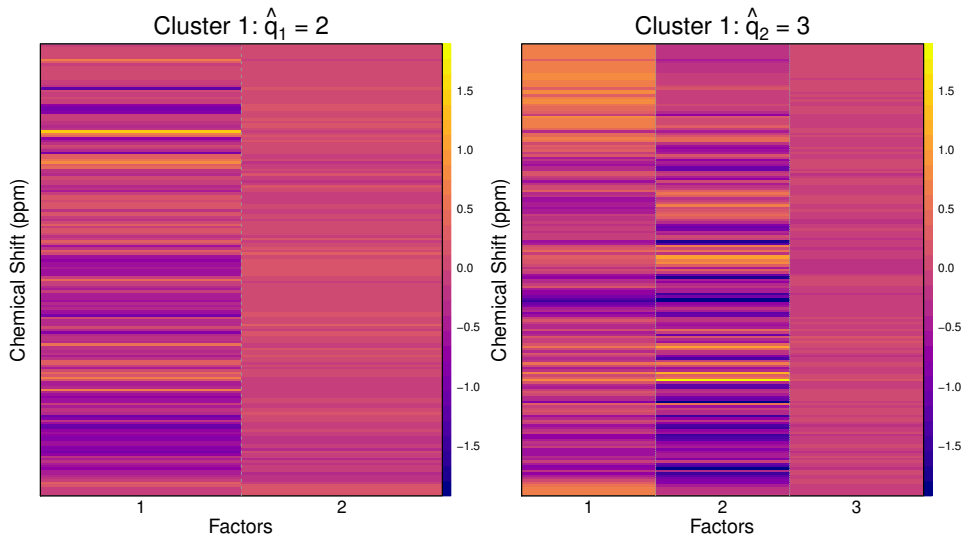


Figure 6: Heat maps, calibrated to a common colour scale, of the posterior mean loadings matrices in the 2 clusters uncovered by the MIFA model applied to the spectral metabolomic data. Darker colours correspond to more negative entries, and *vice versa*.

However, just one run of IMIFA, with sufficiently strong shrinkage hyperparameters and the PYP prior, is unanimous in visiting a 3-cluster model with $\hat{q}_g = 2 \ \forall \ g$. The MAP clustering uncovers the clustering structure perfectly, save for the same epileptic participant misclassified by MIFA now being given its own cluster (see Table 4), yielding an adjusted Rand index of 0.89 and error rate of 5.56%. Examination of covariates associated with the study participants reveals the lone epileptic participant to have an abnormally low weight, quite distinct from all study participants. Furthermore, the absence of the outlier in the epileptic cluster may account for the estimate of q_g therein now being 2, rather than 3 as it was under MIFA. Notably, IMIFA’s performance also compares favourably to OMIFA’s 2-cluster solution (adjusted Rand index = 0.08; error rate = 33.33%), although fitting OMIFA is more computationally efficient taking around three quarters of the time taken for the IMIFA run. Computation times for MIFA and MFA are 1.16 and 1.57 times greater than the single IMIFA run, respectively, showing the benefits of the simplification of the model search under IMIFA.

Table 4: Cross tabulation of the IMIFA model’s MAP $G = 3$ clustering (columns) against true group membership (rows) for the spectral metabolomic data.

	1	2	3
Control	9	0	0
Epileptic	0	8	1

Posterior predictive checks of the IMIFA model fit are shown in Figure 7 which illustrates the discrepancy between the empirical and estimated covariance matrices through a range of error metrics and their associated uncertainty. Given the large number of covariance parameters being compared, the vast majority of the deviations being close to zero suggests the IMIFA model fits well.

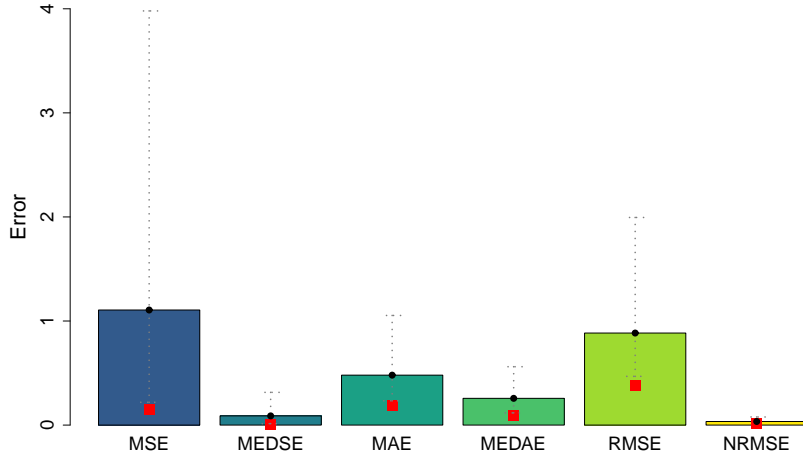


Figure 7: Discrepancies between empirical and estimated covariance matrices for IMIFA fitted to the metabolomic data. Mean and median squared error (MSE/MEDSE), mean and median absolute error (MAE/MEDAE), root mean squared error (RMSE) and normalised root mean squared error (NRMSE) are illustrated. The NRMSE is the RMSE divided by the empirical covariance matrix range (25.64 here) and thus is a proportion. The height of each bar gives the average value of the respective metric (NRMSE \approx 0.035), while the red square gives the metric at the parameters’ posterior means (NRMSE \approx 0.015). 95% credible intervals are shown via dotted grey lines.

3.4 Manifold Learning: Handwritten Digit Recognition Data

A final illustration of IMIFA is given through its application to well known handwritten digit data from the United States Postal Service (USPS) (Hastie et al., 2001). Here the training data are considered, comprising 7,291 images of the digits 0,...,9, taken from handwritten zip codes. Each digit is represented by a 16×16 grayscale grid concatenated into a 256-dimensional vector. Such data are often considered in the context of manifold learning, positing that the dimensionality of the data is artificially high. Due to the size and dimensionality of the USPS data, fitting MFA models over a range of G and q values – indeed even running a range of MIFA models – is practically infeasible. Thus, results of a single IMIFA run are presented here. It is anticipated that the flexibility afforded by IMIFA, in particular allowing cluster-specific numbers of factors, will help characterise digits with different geometric features and complexities.

All hyperparameter settings are as discussed previously, with the exception of the adoption of a flatter prior on the cluster means, given the variation across the images: $\underline{\mu}_g \sim \text{MVN}_p(\tilde{\underline{\mu}}, 10^3 \tilde{\Sigma})$. Cluster allocations were initialised using k -means and data were not standardised. Pixels around the edges of the images (with standard deviation < 0.7 , remaining mostly white across all images) were discarded as such pixels are unlikely to be discriminatory given the geometry of the digits (Bouveyron & Brunet-Saumard, 2014) but may reduce performance; the IMIFA robustness study (see Appendix B) suggests that clustering performance disimproves as the signal-to-noise ratio decreases.

Table 5: Cross tabulation of IMIFA’s MAP clustering (rows) against the true digit labels (columns) for the USPS data. Cells that are 0 are left blank for clarity. Posterior mean cluster proportions $\hat{\pi}_g$ and the modal estimate of the cluster-specific number of factors \hat{q}_g , with associated 95% credible intervals in brackets, are also given.

	0	1	2	3	4	5	6	7	8	9	$\hat{\pi}_g$	\hat{q}_g
1	441										0.06	5 [4, 5]
2		821			2						0.11	2 [1, 4]
3			245	7	1	1	3	39		2	0.04	7 [6, 8]
4	72		13	109		84	7		32		0.04	6 [5, 9]
5				145							0.02	2 [1, 3]
6	12		1	223		179				1	0.06	6 [4, 7]
7						1	389				0.05	5 [4, 6]
8								395			0.05	3 [2, 4]
9	22	18	5	19	5	14	19	8	308	12	0.06	7 [6, 8]
10		11		1	83	1		128	2	373	0.08	4 [3, 5]
11			180		2		1				0.02	5 [4, 7]
12	188	2	194	105	146	94	77	6	198	38	0.15	11 [8, 14]
13	29		93	2	35	13	1	1			0.02	5 [4, 6]
14		152							1		0.02	2 [1, 3]
15						163	3				0.02	6 [5, 7]
16		1		1	267	1		50	1	195	0.07	5 [4, 6]
17							164				0.02	5 [3, 6]
18	430										0.06	5 [4, 7]
19					111	1		18		23	0.02	5 [4, 6]
20				46		4					0.01	2 [1, 4]

The IMIFA model suggests $\hat{G} = 20$ (with 95% credible interval: $G \in [20, 21]$); Table 5 cross-tabulates the MAP clustering against the known digit labels, from which the digit captured by each cluster can be roughly identified. Intuitively, IMIFA assigns images of the same digit, albeit written differently, to different clusters. Plots of the posterior mean of clusters 2 and 14, clusters 3 and 11, and clusters 9 and 12 are shown in Figure 8; additional plots relating to the application of IMIFA to these data are deferred to Appendix C.

Clusters 2 and 14 appear to capture the digit 1 either written in a straight or slanted fashion, respectively. Clusters 3 and 11 appear to represent two different ways of writing the digit 2: with a loop (cluster 3) or with a straight pivot (cluster 11). Notably cluster 3, which represents a more geometrically complex way of writing the digit 2, requires more factors than cluster 11. Clusters 9 and 12 appear to represent the digit 8 and require a large number of factors ($\hat{q}_9 = 7, \hat{q}_{12} = 11$) in comparison, say, to clusters 2 and 14 ($\hat{q}_2 = \hat{q}_{14} = 2$) which capture the digit 1. This is intuitive, as the digit 8 is more geometrically complex than the digit 1. Furthermore, Table 5 indicates that cluster 12 also captures several images of other digits, all of which are reflected in the resulting posterior mean image and in the fact that \hat{q}_{12} is the largest among all clusters.

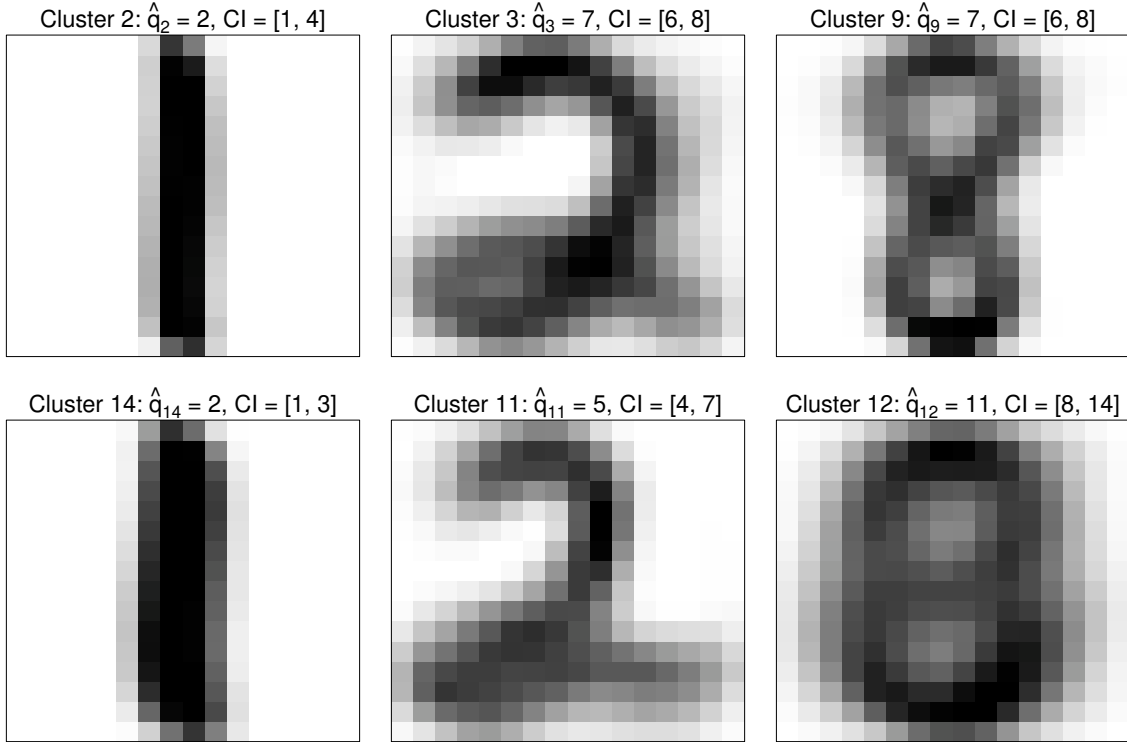


Figure 8: Posterior mean images for a selection of clusters uncovered by IMIFA fitted to the USPS data. Plots are labelled with the cluster index, the modal number of cluster-specific factors (with associated 95% credible intervals in brackets).

Overall, assuming a factor-analytic mixture is to be fitted for clustering purposes, the simulation study and range of applications strongly and clearly demonstrate the flexibility, model search simplification, computational efficiency, and clustering accuracy of the flagship IMIFA model, which requires little user intervention.

4 Discussion

The infinite mixture of infinite factor analysers model, a Bayesian nonparametric approach to clustering high-dimensional data using mixture models with a factor-analytic structure, has been introduced herein. The IMIFA model sidesteps the fraught and computationally intensive task of determining the optimal number of clusters and factors by allowing infinitely many of both. The proposed IMIFA model seamlessly and

flexibly achieves clustering while allowing factor-analytic models of different dimensions in different clusters, without the need for model selection criteria. A Pitman-Yor process mixture model provides the infinite mixture structure in IMIFA, and multiplicative gamma process shrinkage priors on the cluster-specific loadings matrices provide the potentially infinite number of latent factors, thereby generalising and extending the MGP prior (Bhattacharya & Dunson, 2011). This modelling flexibility has been shown to have the potential to notably improve clustering results, while facilitating quantification of the uncertainty in both the numbers of clusters and cluster-specific factors. Furthermore, a full flexible family of IMIFA related models including versions in which the mixture is finite or overfitted, and versions in which the number of factors is finite or infinite, have been described and proposed. The link between factor analysis and PPCA has also been explored, and developed in the context of the IMIFA family of models. Inference across the family of models is efficiently achieved by Gibbs sampling, with use of the independent slice-efficient sampler depending on the model under consideration, with Metropolis-within-Gibbs steps required when the PYP prior is assumed.

The performance of the family of IMIFA related models, and the excellent performance of the IMIFA model in particular, are demonstrated via application to simulated data, to a benchmark data set of Italian olive oils, to real data from a metabolomics based study on epilepsy, and to handwritten digit recognition data. In all cases the IMIFA model proves to be a computationally efficient, flexible, and accurate approach to clustering data without reliance on model selection criteria, by virtue of the simplification of the model search it achieves. The advantage of the flexibility of the cluster-specific number of factors is borne out in the applications resulting in improved clustering results, as is the benefit of the quantifying the uncertainty in the numbers of clusters and cluster-specific factors. Posterior predictive checking has been proposed and employed to assess the fit of IMIFA related models. The full IMIFA family of models can be efficiently fitted through the open source R software environment: the **IMIFA** package is available from www.r-project.org (Murphy et al., 2017; R Core Team, 2017).

Sensitivity to the PYP parameters and initial allocations has been comprehensively explored and sensible priors for the component means, factor scores, and uniquenesses have been proposed; the same is true of the MGP prior on the factor loadings, with sensible hyper-priors on the local and global shrinkage parameters. However, as with all Bayesian specifications of factor-analytic models, and mixtures thereof, poor hyperparameter settings may introduce additional clusters or factors to maintain flexibility in characterising the joint distribution of the data. In particular, the influence of the prior on the cluster means can be notable, especially in cases in which cluster means are quite distinct and/or the data have not been standardised prior to analysis. Thus, employing a flat MVN prior via an inflated covariance matrix (here by considering small values of the parameter φ) is recommended. As such, care is advised when specifying priors or starting values for IMIFA related models, as is typical of Bayesian analyses.

Future research directions are varied and plentiful and other modelling complexities could be incorporated within the IMIFA family of models. For example, covariates could be incorporated in the spirit of Bayesian factor regression models (West, 2003; Carvalho et al., 2008). Such an approach would allow for direct inclusion of the weight and urine pH covariates available with the spectral metabolomic data considered in Section 3.3, for example. Furthermore, the models could be extended to be applicable

in supervised or semi-supervised settings where some or all of the data are labelled, in order to facilitate their use in supervised or semi-supervised model-based classification. For many applied problems, the tails of the normal distribution are often shorter than required: considering the family of IMIFA models with the multivariate t -distribution (Peel & McLachlan, 2000) as an alternative to the underlying multivariate Gaussian distribution, would provide further model flexibility. As ever, the robustness to outliers this would afford could inhibit overestimation of the number of clusters when the assumption of component multivariate normality is not satisfied. Moreover, concerns regarding model misspecification raise queries on the guarantee of posterior consistency for the number of components, which is contingent on correct specification of the family of component distributions. Miller & Harrison (2014) clearly demonstrate this concern for mixtures of Gaussians and suggest that to reliably assess heterogeneity the effects of model misspecification must be considered; approaches such as that of Woo & Sriram (2006) may be fruitful. These concerns highlight the need by practitioners to pay due consideration to the uncertainty in the number of components offered by IMIFA.

While inference on the family of IMIFA related models has been demonstrated to be efficient and practically feasible, there is scope for further finessing. Implementation of the third label switching move of Hastie et al. (2014), exploration of the utility of the collapsed Gibbs sampler (Yu, 2009) or of posterior tempering to encourage better early mixing are all of potential interest; Papastamoulis (2018) uses prior parallel tempering in a closely related overfitted setting, albeit with finite factors. Furthermore, as proposed by Bhattacharya & Dunson (2011), the hyperparameters of the MGP shrinkage prior could be learned from the data rather than fixed as in the IMIFA family of models considered here. However, such learning requires introducing extra Metropolis-Hastings steps which would computationally impact the fitting of IMIFA.

Acknowledgements

This research emanated from work conducted with the financial support of Science Foundation Ireland under grant number SFI/12/RC/2289 in the Insight Centre for Data Analytics in University College Dublin (UCD).

The authors wish to thank the members of the UCD Working Group in Statistical Learning and the members of Prof. Adrian Raftery’s Working Group in Model-based Clustering for helpful discussion and feedback. The authors also thank Prof. Lorraine Brennan at the UCD Institute of Food and Health for providing the spectral metabolomic data.

Appendices

A Posterior Conditional Distributions: Technical details for sampling from the IMIFA model

The structure of the Metropolis-within-Gibbs sampler to conduct inference for the IMIFA model and the exact parameterisations of the required conditional distributions are detailed below. Note that $\text{Ga}(\alpha, \beta)$ refers throughout to the gamma distribution with mean α/β . Algorithms for sampling other models in the IMIFA related family can all be considered as special cases of what follows. The algorithm is implemented in the associated R package **IMIFA** (Murphy et al., 2017).

For $g = 1, \dots, \tilde{G}$, where \tilde{G} is the current sample of the number of active clusters and \tilde{q}_g is the current sample of the number of active factors:

$$\begin{aligned}
\underline{\mu}_g &| \dots \sim \text{MVN}_p \left(\Omega_{\underline{\mu}_g}^{-1} \left(\Psi_g^{-1} \left(\sum_{i:z_{ig}=1} \underline{x}_i - \sum_{i:z_{ig}=1} \Lambda_g \underline{\eta}_i \right) + \varphi \tilde{\Sigma}^{-1} \tilde{\underline{\mu}} \right), \Omega_{\underline{\mu}_g}^{-1} \right) \\
\underline{\eta}_{i:z_{ig}=1} &| \dots \sim \text{MVN}_{\tilde{q}_g} \left(\Omega_{\underline{\eta}_g}^{-1} \Lambda_g^\top \Psi_g^{-1} (\underline{x}_{i:z_{ig}=1} - \underline{\mu}_g), \Omega_{\underline{\eta}_g} \right) & \text{for } i = 1, \dots, n_g \\
\underline{\Lambda}_{jg} &| \dots \sim \text{MVN}_{\tilde{q}_g} \left(\Omega_{\underline{\Lambda}_{jg}}^{-1} \eta_{i:z_{ig}=1}^\top \psi_{jg}^{-1} (\underline{x}_{i:z_{ig}=1}^{(j)} - \mu_{jg}), \Omega_{\underline{\Lambda}_{jg}}^{-1} \right) & \text{for } j = 1, \dots, p \\
\psi_{jg} &| \dots \sim \text{IG} \left(\alpha + \frac{n_g}{2}, \beta_j + \frac{\mathcal{S}_{jg}}{2} \right) & \text{for } j = 1, \dots, p \\
\phi_{jkg} &| \dots \sim \text{Ga} \left(\nu + \frac{1}{2}, \varrho + \frac{\tau_{kg} \lambda_{jkg}^2}{2} \right) & \begin{array}{l} \text{for } j = 1, \dots, p \\ k = 1, \dots, \tilde{q}_g \end{array} \\
\delta_{1g} &| \dots \sim \text{Ga} \left(\alpha_1 + \frac{p\tilde{q}_g}{2}, \beta_1 + \frac{1}{2} \sum_{h=1}^{\tilde{q}_g} \tau_{hg}^{(1)} \sum_{j=1}^p \lambda_{jhg}^2 \phi_{jhg} \right) \\
\delta_{kg} &| \dots \sim \text{Ga} \left(\alpha_2 + \frac{p}{2} (\tilde{q}_g - k + 1), \beta_2 + \frac{1}{2} \sum_{h=k}^{\tilde{q}_g} \tau_{hg}^{(k)} \sum_{j=1}^p \lambda_{jhg}^2 \phi_{jhg} \right) & \text{for } k = 2, \dots, \tilde{q}_g \\
v_g &| \dots \sim \text{Beta} \left(1 - d + n_g, \alpha + gd + N - \sum_{l=1}^g n_l \right) \\
u_i &| z_{ig} = 1, \dots \sim \text{Unif} (0, \xi_g) & \text{for } i = 1, \dots, N
\end{aligned}$$

where

$$\begin{aligned}
\Omega_{\underline{\mu}_g} &= \varphi \tilde{\Sigma}^{-1} + n_g \Psi_g^{-1} \\
\Omega_{\underline{\eta}_g} &= \mathcal{I}_{\tilde{q}_g} + \Lambda_g^\top \Psi_g^{-1} \Lambda_g \\
\Omega_{\underline{\Lambda}_{jg}} &= \text{diag} \left(\phi_{j1g} \tau_{1g}, \dots, \phi_{j\tilde{q}_gg} \tau_{\tilde{q}_gg} \right) + \psi_{jg}^{-1} \eta_{i:z_{ig}=1}^\top \eta_{i:z_{ig}=1} \\
\underline{x}^{(j)} &\text{ denotes the } j\text{-th column of the data matrix} \\
\lambda_{jkg}^2 &\text{ is a single squared loading}
\end{aligned}$$

$$\tau_{kg} = \prod_{h=1}^k \delta_{hg} \text{ is updated after every update of } \delta_{hg}$$

$$\tau_{hg}^{(k)} = \prod_{t=1}^h \frac{\delta_{tg}}{\delta_{kg}}$$

$$\pi_g = v_g \prod_{l=1}^{g-1} (1 - v_l)$$

and

$$\mathcal{S}_{jg} = \sum_{i:z_{ig}=1} (x_{ij} - \mu_{jg} - \underline{\Lambda}_{jg} \underline{\eta}_i)^\top (x_{ij} - \mu_{jg} - \underline{\Lambda}_{jg} \underline{\eta}_i)$$

Notably, if uniquenesses are constrained to be isotropic, such that $\Psi_g = \text{diag}(\psi_g, \dots, \psi_g)$, leading IMIFA to actually correspond to an extension of probabilistic principal component analysis (Tipping & Bishop, 1999) to an infinite mixture context, then

$$\psi_g \mid \dots \sim \text{IG} \left(\alpha + \frac{pn_g}{2}, \beta + \frac{\text{tr}(\mathcal{S}_g)}{2} \right)$$

Uniquenesses can also be constrained across clusters, with or without the isotropic constraint.

In the contexts of finite and overfitted mixtures (i.e. MFA, MIFA, OMFA, and OMIFA):

$$\underline{z}_i \mid \underline{x}_i, \dots \sim \text{Mult} (1, p_1, \dots, p_{\tilde{G}})$$

with
$$\underline{p}_g = \text{P} \left(z_{ig} = 1 \mid \underline{x}_i, \dots \right) = \frac{\pi_g f \left(\underline{x}_i \mid \underline{\mu}_g, \Lambda_g \Lambda_g^\top + \Psi_g \right)}{\sum_{g=1}^{\tilde{G}} \pi_g f \left(\underline{x}_i \mid \underline{\mu}_g, \Lambda_g \Lambda_g^\top + \Psi_g \right)}$$

whereas under the IMFA and IMIFA models:

$$z_{ig} = 1 \mid \dots \propto f \left(\underline{x}_i \mid \underline{\mu}_g, \Lambda_g \Lambda_g^\top + \Psi_g \right) \frac{\pi_g}{\xi_g} \mathbb{1} \left(u_i < \xi_g \right)$$

Sampling is performed in an efficient, numerically stable fashion in both cases, using the unnormalised log-probabilities and i.i.d. draws from the standard Gumbel distribution (Yellott, 1977) via $-\ln(m_{ig})$, with $m_{ig} \sim \text{Exp}(\lambda = 1)$. Observation i is assigned the label g satisfying

$$\arg \max_{g \in \{1, \dots, \tilde{G}\}} \left\{ \ln(p_{ig}) - \ln(m_{ig}) \right\}$$

For the IMIFA and IMFA models, the sampler need only find the maximum over, and only draw Gumbel noise for, log-probabilities for which the indicator function above evaluates to 1.

Sampling the parameters of the PYP for non-zero d values necessitates the introduction of Metropolis-Hastings steps within the Gibbs sampler. Firstly, the hyper-prior assumed for the discount parameter d is similar to the one assumed by (Carmona et al., 2018); a mixture of a point-mass at zero and a continuous beta distribution, in order to consider the DP special case where $d = 0$ with positive probability, i.e. $d \sim \kappa \delta_0 + (1 - \kappa) \text{Beta}(d \mid a', b')$, thus facilitating explicit comparison between DP models and encompassing PYP alternatives. Secondly, the hyper-prior for the α parameter is given conditionally on d , s.t. $\alpha \mid d \sim \text{Ga}(\alpha + d \mid a, b)$, and includes the constraint that $\alpha > -d$ by shifting the support of the gamma density to the interval $(-d, \infty)$.

The likelihood for α and d is given by the exchangeable partition probability function induced by the Poisson-Dirichlet process (Pitman, 1995). Thus the conditional posterior distributions of these parameters are:

$$\begin{aligned} \alpha \mid d, \dots &\propto \frac{\Gamma(\alpha + 1)}{\Gamma(\alpha + N)} \left\{ \prod_{g=1}^{G_0-1} (\alpha + gd) \right\} p(\alpha \mid d) \\ d \mid \alpha, \dots &\propto \left\{ \prod_{g=1}^{G_0-1} (\alpha + gd) \right\} \left\{ \prod_{g=1}^{G_0} \frac{\Gamma(n_g - \alpha)}{\Gamma(1 - \alpha)} \right\} p(d) \end{aligned}$$

Sampling from these distributions, while always considering the support $\alpha > -d$, proceeds as per (Carmona et al., 2018); a Metropolis-Hastings step is implemented for the discount parameter with independent proposal distribution $0.5\delta_0 + 0.5\text{Beta}(d | 1, 1)$, and a random walk Metropolis-Hastings step with proposal distribution given by $\alpha^* | \alpha \sim \text{Unif}(\alpha - \zeta, \alpha + \zeta)$ is implemented for the concentration parameter, where ζ ($= 2$ in our implementation) is used to control the acceptance rate. For the discount parameter, the mutation rate is considered rather than the acceptance rate, whereby a move is only considered accepted if the proposal differs from the current value.

However, when the DP prior is assumed, or when the sampled value of d is exactly zero under the PYP prior, α is updated according to the auxiliary variable routine of (West, 1992), with Gibbs updates by simulation from a weighted mixture of two gamma distributions, as below:

$$\alpha | G_0, \chi, \dots \sim \omega_\chi \text{Ga}(a + G_0, b - \ln(\chi)) + (1 - \omega_\chi) \text{Ga}(a + G_0 - 1, b - \ln(\chi))$$

where G_0 denotes the number of non-empty clusters

and $\chi | \alpha, G_0 \sim \text{Beta}(\alpha + 1, N)$

with mixing weights ω_χ defined by

$$\frac{\omega_\chi}{1 - \omega_\chi} = \frac{(a + G_0 - 1)}{N(b - \ln(\chi))}$$

B Assessing Robustness of the IMIFA Model

In order to assess the robustness of the IMIFA model, $N(0, 1)$ noise with no clustering information was appended separately to the rows and columns of the olive oil data set. Six new scenarios were generated with 10, 50, and 100 extra variables, and the same numbers of extra observations. Cluster validity is evaluated in Table 6 with respect to the new 4-area relabelling in Table 3b. In the case of extra observations, noise observations are labelled as though they belong to a fifth group. Data were mean-centered and unit scaled only after expansion.

As the number of irrelevant variables increases, the clustering structure can still be uncovered quite well, however mixing becomes slower and there is increasing support for a 1-group, 1-factor model as the signal-to-noise ratio decreases. As such, variable selection, or at least the need to pre-process the data, may still be required. As rows of noise are appended, the IMIFA model generally has no difficulty in assigning these observations to a cluster of their own, but their presence leads to overestimation of the total number of clusters, yielding a poorer (though still homogeneous) clustering overall.

Table 6: Clustering performance of the IMIFA model on expanded noisy versions of the Italian olive oil data set. The run time relative to the IMIFA run on the original olive oil data, the posterior mean of the PYP parameters α and d , the modal estimates of G and \underline{Q} , and the adjusted Rand index and misclassification error rate are detailed.

Scenario	Rel. Time	α	d	G	\underline{Q}	Adj. Rand	Error(%)
N=572, p=18	1.16	0.97	0.01	5	2, 2, 2, 2, 2	0.96	6.64
N=572, p=58	2.89	0.98	0.01	5	2, 1, 1, 1, 2	0.85	10.49
N=572, p=108	5.83	1.09	0.02	5	2, 1, 1, 1, 2	0.74	14.69
N=582, p=8	1.06	0.99	0.01	5	2, 1, 1, 2, 1	0.94	6.87
N=622, p=8	1.08	0.96	0.01	5	3, 1, 1, 1, 1	0.94	6.59
N=672, p=8	1.09	0.92	0.01	5	3, 1, 1, 1, 1	0.95	6.40

C Additional Results and Visualisations

In this Section, additional visualisations of the results of the illustrative applications are provided. Specifically, uncertainty in the allocation of observations to components is discussed with reference to the olive oil data, convergence and mixing issues are assessed visually for the spectral metabolomic data, and posterior predictive checking is conducted for the USPS data. All plots were produced using the associated R package **IMIFA** (Murphy et al., 2017).

C.1 Olive oil data

Figure C.1 shows the trace plot of the number of active clusters \tilde{G} (for which parameters are sampled) proposed by the independent slice-efficient sampler for the IMIFA model fitted to the olive oil data set, after accounting for burn-in and thinning. The trace of the non-empty subset G_0 , with which the true number of clusters is inferred, is also depicted.

The modal estimate of the number of non-empty clusters is $\hat{G} = 4$. Regarding the uncertainty in the allocations to these 4 clusters, the uncertainty with which observation i is assigned to its cluster is estimated by

$$U_i = \min_{g=1,\dots,\hat{G}} \{1 - \mathbb{P}(\text{cluster } g \mid \text{observation } i)\}$$

Figure C.2 illustrates the clustering uncertainties under the IMIFA model fitted to the olive oil data set. In arriving at these estimates, only iterations where a 4-cluster solution was visited were considered. The maximum uncertainty observed is 0.236, corresponding to the lone incorrectly clustered Sardinian observation; thus while this observation is wrongly assigned to Cluster 3, it has large probability of belonging to the other clusters under the IMIFA model.

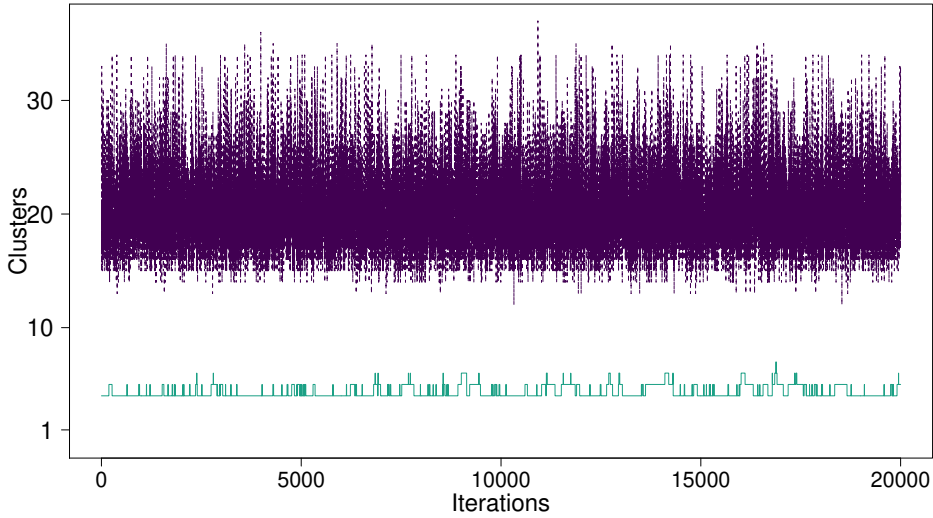


Figure C.1: Trace of the active clusters (above) and the non-empty subset (below) visited by the IMIFA model fitted to the olive oil data set, after accounting for burn-in and thinning.

As an alternative means of summarising the clustering of the IMIFA model fitted to the olive oil data set, a heatmap of the ‘average’ similarity matrix is shown in Figure C.3. At each iteration of the MCMC sampler, $N \times N$ adjacency matrices are created from the sampled cluster labels and stored. These contain a 1 in position ij if observations i and j are clustered together, and zero otherwise. After the sampler has finished running, the similarity matrix is computed as the average of all the stored adjacency matrices (Carmona et al., 2018). A desirable feature of this approach is that it uses sampled partitions which need not have the

same number of non-empty clusters, and is invariant to cluster labelling. The clear 4-cluster solution seen here corresponds well to the uncovered MAP clustering; indeed, following the suggestion in [Carmona et al. \(2018\)](#) that the partition can be summarised by the adjacency matrix from the iteration with minimum mean-squared distance from the average similarity matrix, the summary partition obtained in this manner is found to be identical in this instance to the MAP partition.

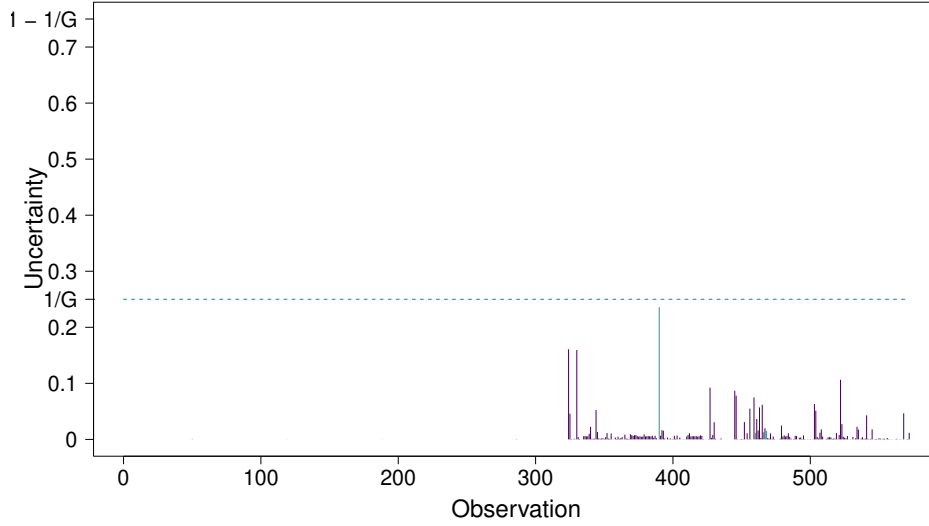


Figure C.2: Observation-specific clustering uncertainties for the IMIFA model fitted to the olive oil data set, with the number of clusters estimated as 4. The lone misclassified observation, according to the new labelling in Table 3b, is highlighted in green.

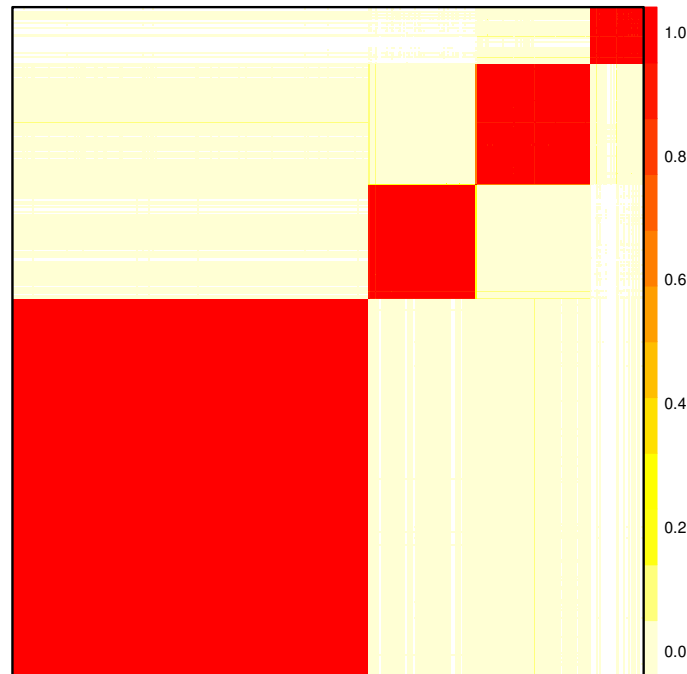


Figure C.3: Average cluster similarity matrix for the IMIFA model fitted to the olive oil data set. Observations have been reordered to correspond to the known group membership labels. Darker colours represent higher probability of two observations belonging to the same cluster, and *vice versa*.

C.2 Spectral metabolomic data

Mixing and convergence for the application of IMIFA to the spectral metabolomic data are assessed visually. Figure C.5 gives, as an example, the trace, posterior kernel density, autocorrelation function (ACF), and partial autocorrelation function (PACF) plots for a single mean parameter for Cluster 1 and Cluster 2 under the IMIFA model fitted to the spectral metabolomic data, after discarding iterations due to burn-in and thinning every 2nd observation. The chains appear to have mixed and converged satisfactorily for both clusters. Figure C.4 gives the posterior mean estimates for all $p = 189$ mean parameters, with 95% credible intervals also depicted. Cluster 3 is not shown in either case as it contains only one subject.

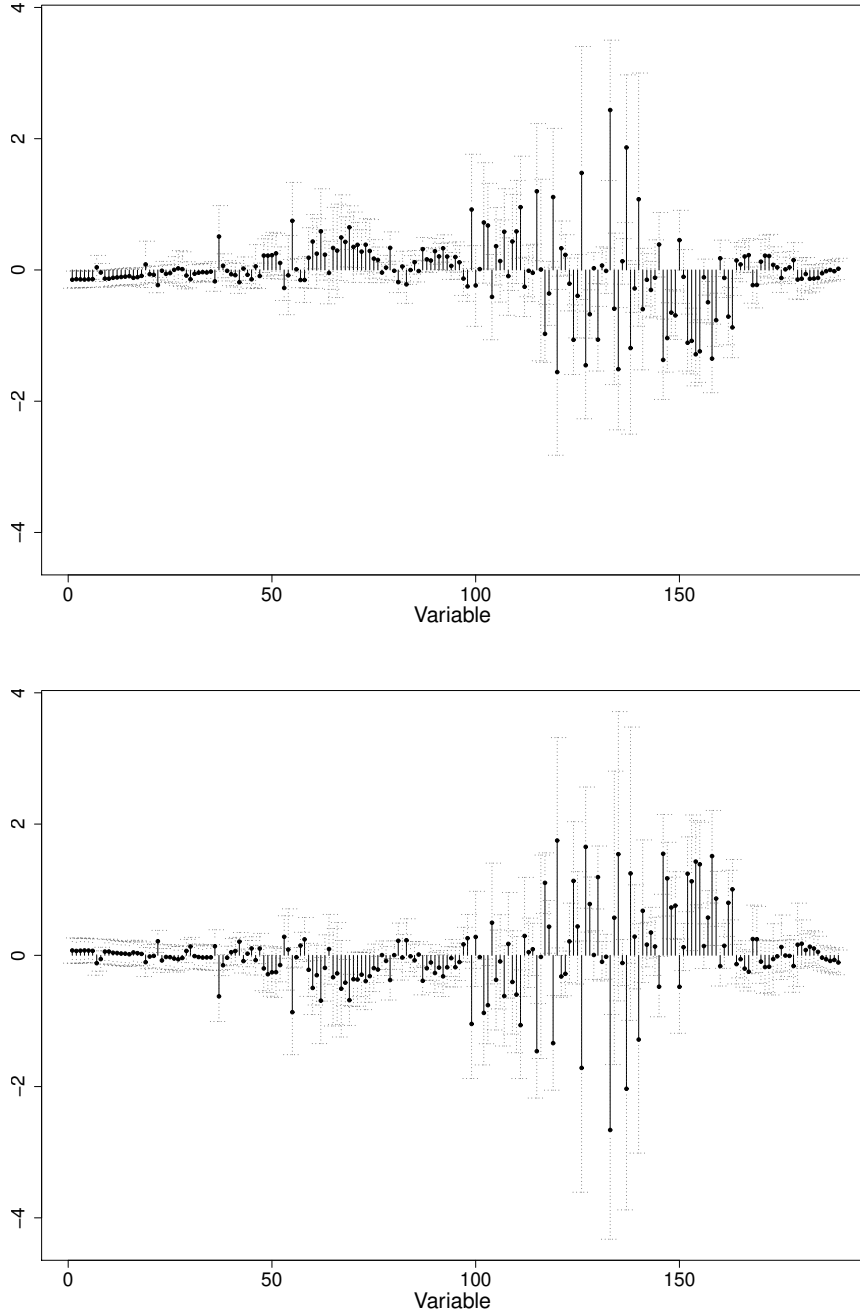
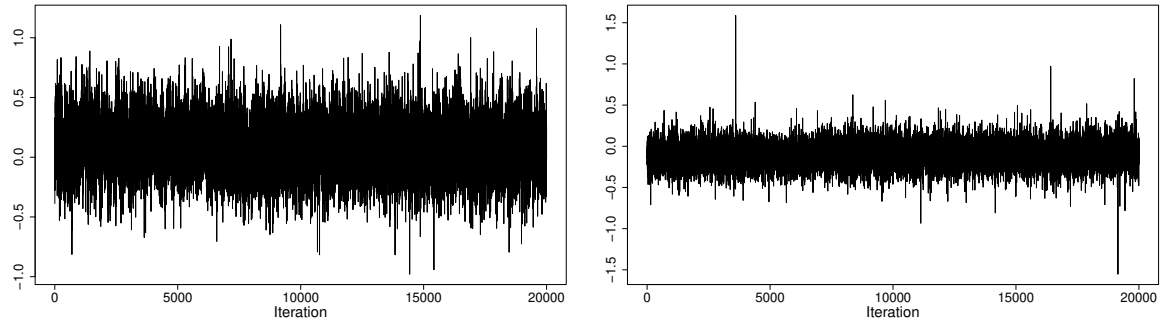
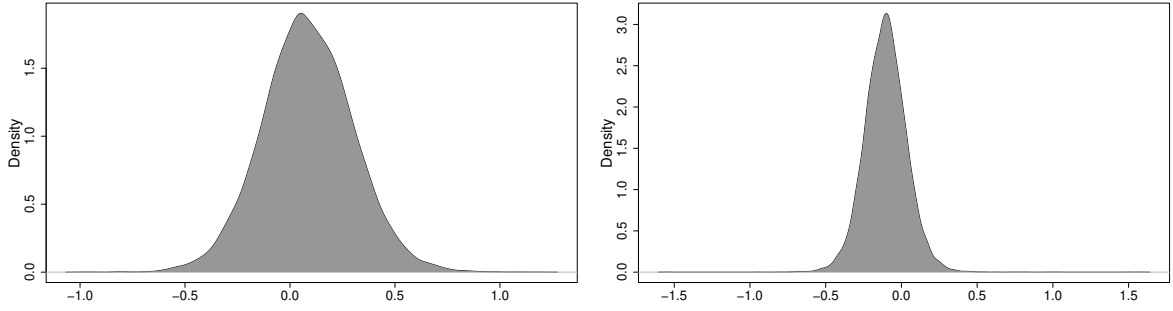


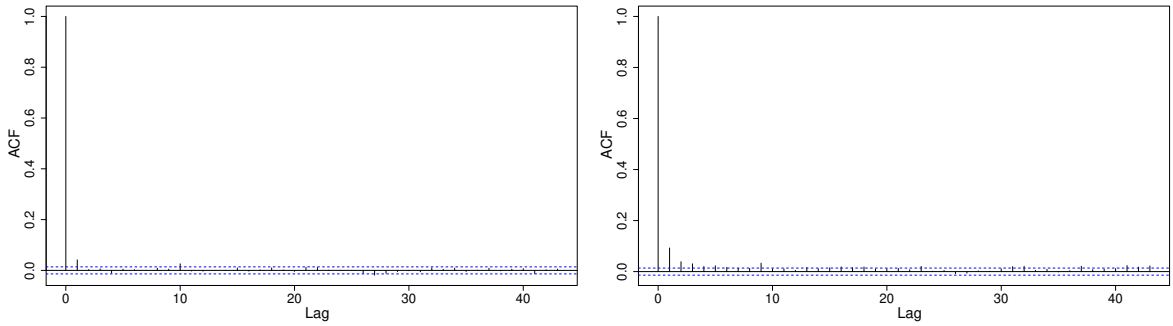
Figure C.4: Posterior mean of all mean parameters of Cluster 1 (above) and Cluster 2 (below) under the IMIFA model fitted to the spectral metabolomic data, with 95% credible intervals given in grey.



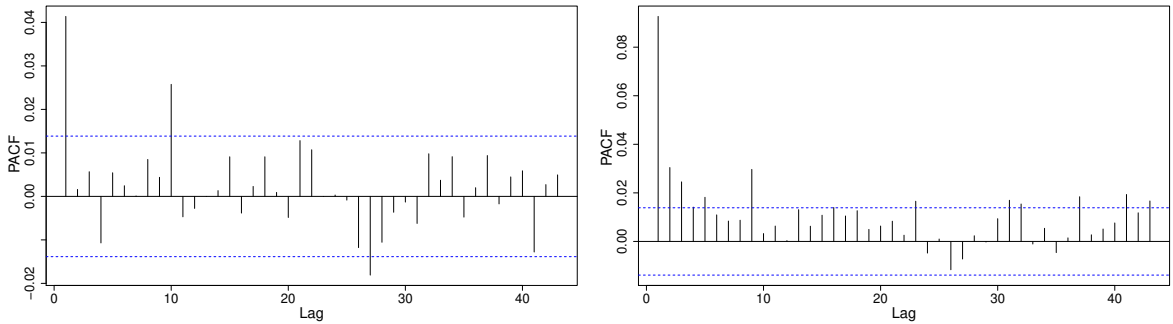
(a) Trace plots.



(b) Kernel density estimates.



(c) ACF.



(d) PACF.

Figure C.5: Trace, kernel density, ACF, and PACF plots for a single mean parameter for Cluster 1 (left) and Cluster 2 (right) under the IMIFA model fitted to the spectral metabolomic data, after discarding iterations due to burn-in and thinning every 2nd observation.

C.3 USPS data

In relation to the USPS handwritten digit data set and the IMIFA model fitted to it, Figure C.6 shows the overall mean of the data and provides justification for the flat prior adopted on the cluster means, while Figures C.7 and C.8 motivate the pre-processing step of discarding peripheral pixels on the basis of their standard deviation.

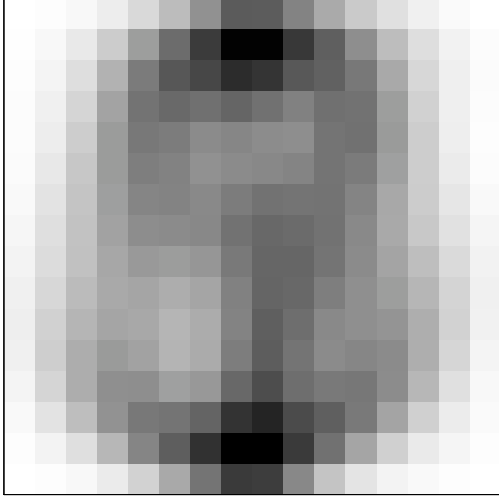


Figure C.6: Overall mean image of the USPS data across all digits and all pixels.

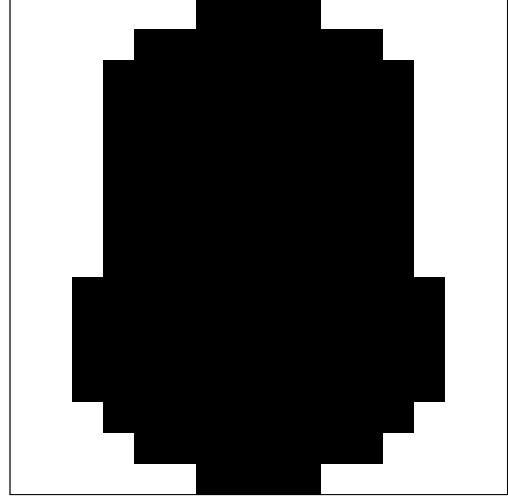


Figure C.7: Pixels retained from the USPS data (in black) after pre-processing.

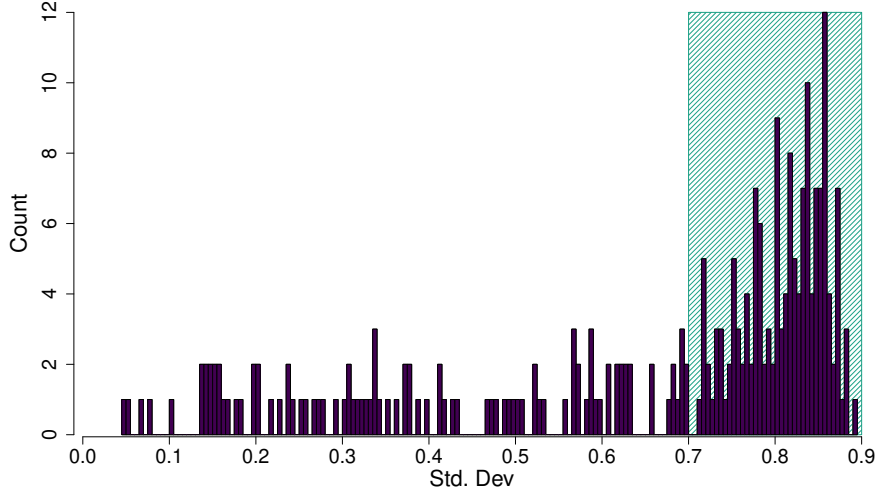


Figure C.8: Histogram of the standard deviations of the pixels in the USPS data. The shaded region corresponds to pixels with standard deviation > 0.7 which were not discarded.

Figure C.9 illustrates measures of discrepancy between the empirical and the estimated covariance matrices. The posterior mean of each of the 20 uncovered clusters are shown in Figure 8. It can be seen, for instance, that Clusters 1 and 18 capture the digit 0 (‘fat’ and ‘skinny’, respectively), while Clusters 7 and 17 capture the digit 6 (with small and big loops, respectively). There is some confusion between the digits 4 and 9 (Clusters 16, 19, and 10). Generally, clusters corresponding to digits which are less geometrically complex require fewer latent factors. Cluster 13 appears to be capturing noise in the data; i.e. correctly capturing digits that should not belong to the other more defined clusters, as they are written differently.

Finally, Figure C.11 represents a heatmap of the average similarity matrix, constructed as per Figure C.3 for the olive oil data application, following Carmona et al. (2018). The clear 20-cluster structure in the set of images is readily apparent, corresponding well to the MAP clustering. It is interesting to note, for instance, that some observations in the first two clusters, which both capture the digit 0 in different ways, have some probability of belonging to the opposite cluster, but no probability of belonging to clusters capturing other digits.

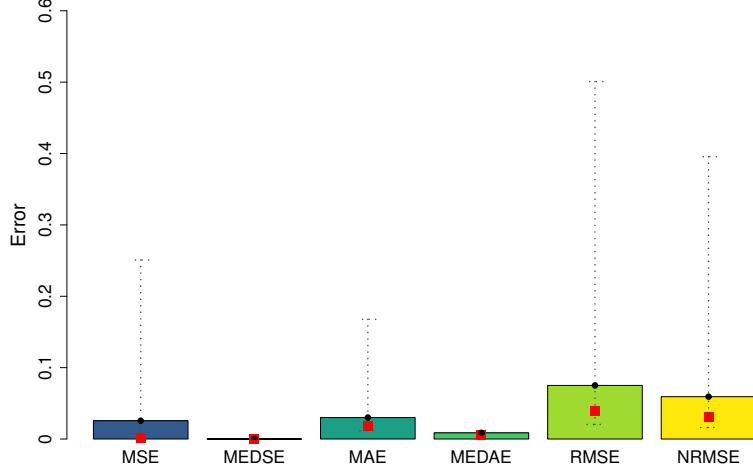


Figure C.9: Measures of discrepancy between the empirical and estimated covariance matrices for the IMIFA model fitted to the USPS data. The height of each bar gives the average value of the respective metric (NRMSE ≈ 0.059), while the red squares give the value evaluated using the posterior mean parameter estimates (NRMSE ≈ 0.031). 95% credible intervals are also shown via dotted grey lines.

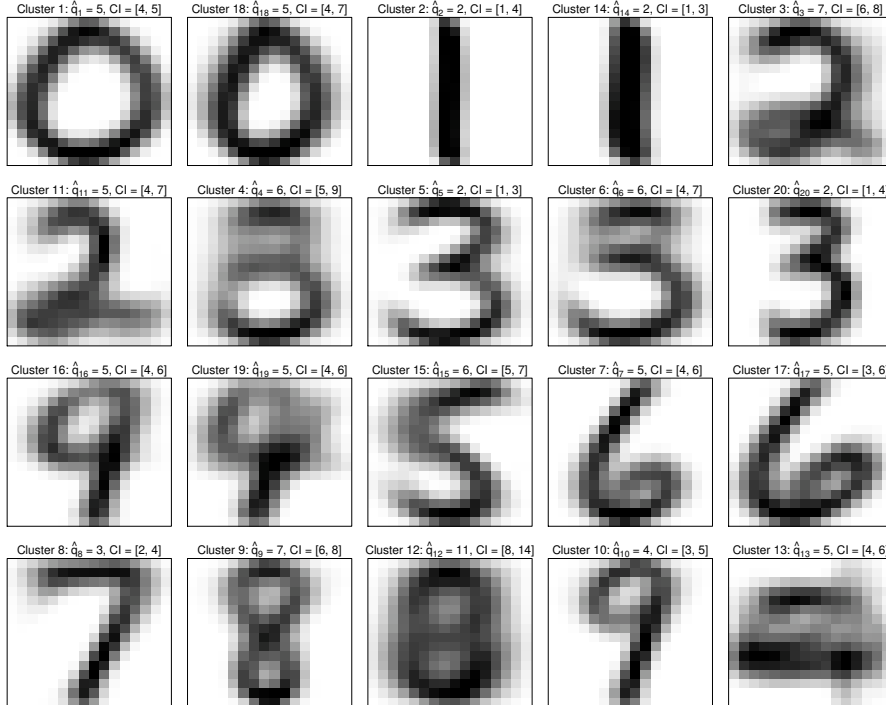


Figure C.10: Posterior mean images for the 20 clusters uncovered by IMIFA fitted to the USPS data, ordered by the digit they most clearly represent (according to the confusion matrix). Plots are labelled with the modal number of factors within that cluster and the associated 95% credible interval.

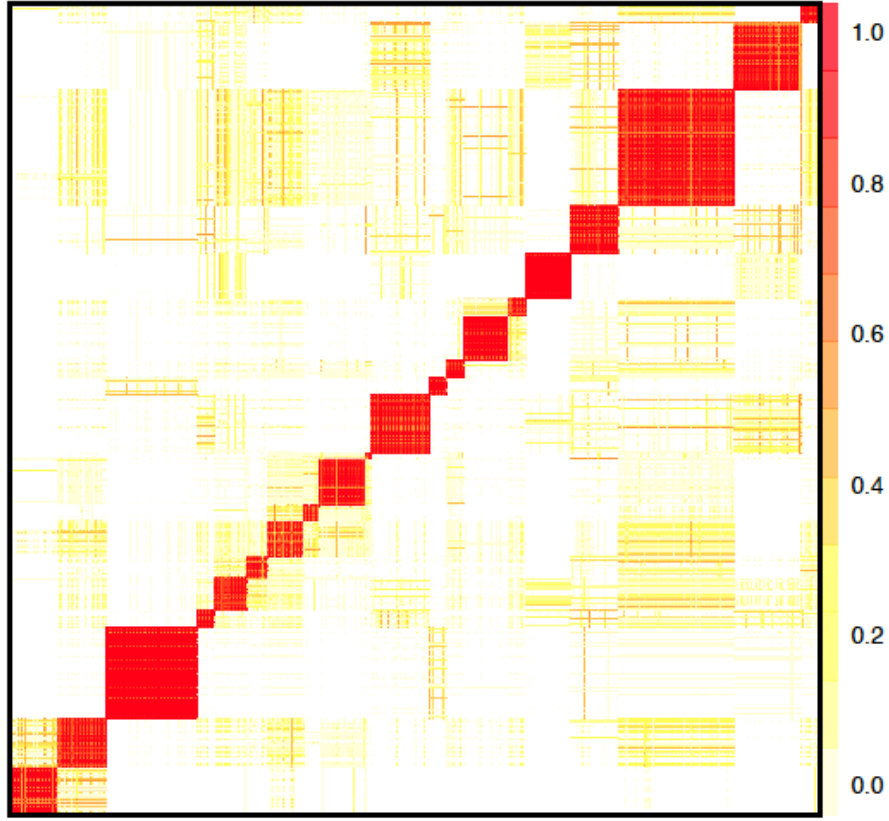


Figure C.11: Average cluster similarity matrix for the IMIFA model fitted to the USPS digit data. Observations have been reordered to correspond to the ordering of the images in Figure C.10. Darker colours represent higher probability of two observations belonging to the same cluster, and *vice versa*.

D Exact Hyperparameter Specifications

Unless otherwise stated in the main text, the exact specifications of the hyper-priors which require selection, for the analyses of the simulated data, olive oil data, spectral metabolomic data, and handwritten USPS data, are as given in Table D.1. Note that these are the default values within the **IMIFA** R package (Murphy et al., 2017). While it may appear that there are many hyperparameters to be chosen, these choices are all reasonably standard. Note that the specification of the beta prior for d here amounts to a standard uniform distribution.

Table D.1: Hyperparameter specifications for the IMIFA model, giving the hyperparameter(s), their value(s), and the parameter(s) to which they pertain.

Parameter(s)	Hyperparameter(s)	Value(s)
$\underline{\mu}_g$	φ	1
$\underline{\psi}_g$	α	2.5
ϕ_{jkg}	(ν, ϱ)	(3, 2)
δ_{1g}	(α_1, β_1)	(2, 1)
δ_{kg}	(α_2, β_2)	(6, 1)
α	(a, b)	(2, 1)
d	(a', b')	(1, 1)

References

- D. Aldous. Exchangeability and related topics. In P. D. Hannequin, editor, *École d'été de probabilités de Saint-Flour XIII–1983*, volume 1117 of *Lecture Notes in Mathematics*, pages 1–198. Springer-Verlag, Berlin, 1985. [10](#)
- A. Ansari, K. Jedidi, & L. Dube. Heterogeneous factor analysis model: a bayesian approach. *Psychometrika*, 67(1): 49–78, 2002. [14](#)
- C. E. Antoniak. Mixtures of dirichlet processes with applications to bayesian nonparametric problems. *The Annals of Statistics*, 2(6): 1152–1174, 1974. [9](#), [10](#)
- J. Baek, G. J. McLachlan, & L. K. Flack. Mixtures of factor analyzers with common factor loadings: applications to the clustering and visualization of high-dimensional data. *IEEE Transactions on Pattern Analysis and Machine Intelligence*, 32(7): 1298–1309, 2010. [2](#)
- J. Bai & K. Li. Statistical analysis of factor models of high dimension. *The Annals of Statistics*, 40(1): 436–465, 2012. [1](#)
- A. Bhattacharya & D. B. Dunson. Sparse bayesian infinite factor models. *Biometrika*, 98(2): 291–306, 2011. [2](#), [3](#), [6](#), [7](#), [23](#), [24](#)
- D. Blackwell & J. B. MacQueen. Ferguson Distributions via Polya Urn Schemes. *The Annals of Statistics*, 1(2): 353–355, 1973. [10](#)
- C. Bouveyron & C. Brunet-Saumard. Model-based clustering of high-dimensional data: A review. *Computational Statistics & Data Analysis*, 71: 52–78, 2014. [21](#)
- S. Carmody & L. Brennan. Effects of pentylene-tetrazole-induced seizures on metabolomic profiles of rat brain. *Neurochemistry International*, 56(2): 340–344, 2010. [18](#)
- C. Carmona, L. Nieto-barajas, & A. Canale. Model based approach for household clustering with mixed scale variables. *Advances in Data Analysis and Classification*, 12: 1–25, 2018. [13](#), [26](#), [27](#), [28](#), [29](#), [33](#)
- G. Carpaneto & P. Toth. Solution of the assignment problem. *ACM Transactions on Mathematical Software*, 6: 104–111, 1980. [5](#)
- C. M. Carvalho, J. Chang, J. E. Lucas, J. R. Nevins, Q. Wang, & M. West. High-Dimensional Sparse Factor Modeling: Applications in Gene Expression Genomics. *Journal of the American Statistical Association*, 103(484): 1438–1456, 2008. [23](#)
- M. Chen, J. Silva, J. Paisley, C. Wang, D. Dunson, & Carin L. Compressive sensing on manifolds using a nonparametric mixture of factor analyzers: Algorithm and performance bounds. *IEEE Transactions on Signal Processing*, 58(12): 6140–6155, 2010. [8](#)
- J. Diebolt & C. P. Robert. Estimation of finite mixture distributions through bayesian sampling. *Journal of the Royal Statistical Society: Series B (Statistical Methodology)*, 56(2): 363–375, 1994. [2](#)
- D. Durante. A note on the multiplicative gamma process. *Statistics & Probability Letters*, 122: 198–204, 2017. [2](#), [6](#), [7](#)
- M. D. Escobar. Estimating normal means with a dirichlet process prior. *Journal of the American Statistical Association*, 89(425): 268–277, 1994. [10](#)

- M. D. Escobar & M. West. Bayesian density estimation and inference using mixtures. *Journal of the American Statistical Association*, 90(430): 577–588, 1995. [10](#)
- T. S. Ferguson. A bayesian analysis of some nonparametric problems. *The Annals of Statistics*, 1(2): 209–230, 1973. [2](#), [9](#)
- E. Fokoué & D. M. Titterington. Mixtures of factor analysers. Bayesian estimation and inference by stochastic simulation. *Machine Learning*, 50(1): 73–94, 2003. [2](#)
- M. Forina, C. Armanino, S. Lanteri, & E. Tiscornia. Classification of olive oils from their fatty acid composition. *Food Research and Data Analysis*, pages 189–214, 1983. [16](#)
- C. Fraley & A. E. Raftery. Model-based clustering, discriminant analysis and density estimation. *Journal of the American Statistical Association*, 97(458): 611–631, 2002. [13](#)
- S. Frühwirth-Schnatter. *Finite Mixture and Markov Switching Models*. Springer series in statistics, 2010. [5](#)
- S. Frühwirth-Schnatter. *Dealing with label switching under model uncertainty*, pages 193–218. Mixture estimation and applications. Wiley, Chichester, 2011. [5](#)
- Frühwirth-Schnatter, S. and Lopes, H. F. Parsimonious bayesian factor analysis when the number of factors is unknown. Technical report, The University of Chicago Booth School of Business, 2010. [4](#)
- A. Gelman, J. B. Carlin, H. S. Stern, D. B. Dunson, A. Vehtari, & D. B. Rubin. *Bayesian Data Analysis*. Chapman and Hall/CRC, 2003. [14](#)
- Z. Ghahramani & G. E. Hinton. The em algorithm for mixtures of factor analyzers. Technical report, Department of Computer Science, University of Toronto, 1996. [1](#), [5](#)
- J. Ghosh & D. B. Dunson. Default Prior Distributions and Efficient Posterior Computation in Bayesian Factor Analysis. *Journal of Computational and Graphical Statistics*, 18(2): 306–320, 2008. [4](#)
- D. I. Hastie, S. Liverani, & S. Richardson. Sampling from Dirichlet process mixture models with unknown concentration parameter: mixing issues in large data implementations. *Statistics and Computing*, 25(5): 1023–1037, 2014. [11](#), [12](#), [24](#)
- T. Hastie, R. Tibshirani, & J. Friedman. *The Elements of Statistical Learning*. Springer Series in Statistics. Springer New York Inc., New York, NY, USA, second edition, 2001. [21](#)
- C. Hennig. Methods for merging gaussian mixture components. *Advances in Data Analysis and Classification*, 4(1): 3–34, 2010. [2](#)
- L. Hubert & P. Arabie. Comparing partitions. *Journal of Classification*, 2(1): 193–218, 1985. [16](#)
- H. Ishwaran, L. F. James, & J. Sun. Bayesian model selection in finite mixtures by marginal density decompositions. *Journal of the American Statistical Association*, 96: 1316–1332, 2001. [9](#), [10](#), [13](#)
- M. Kalli, J. E. Griffin, & S. G. Walker. Slice sampling mixture models. *Statistics and Computing*, 21(1): 93–105, 2011. [2](#), [10](#), [11](#)

- R. E. Kass & A. E. Raftery. Bayes factors. *Journal of the American Statistical Association*, 90(430): 773–795, 1995. [2](#)
- M. Knott & D. J. Bartholomew. *Latent Variable Models and Factor Analysis*. Number 7. Edward Arnold, 1999. [1](#), [4](#)
- D. Knowles & Z. Ghahramani. Infinite sparse factor analysis and infinite independent components analysis. In M. E. Davies, C. J. James, S. A. Abdallah, & M. D. Plumbley, editors, *Independent Component Analysis and Signal Separation*, pages 381–388, Berlin, Heidelberg, 2007. Springer Berlin Heidelberg. [8](#)
- G. J. McLachlan & D. Peel. *Finite mixture models*. Wiley series in probability and statistics. J. Wiley & Sons, New York, 2000. [1](#), [5](#)
- P. D. McNicholas. Model-based classification using latent gaussian mixture models. *Journal of Statistical Planning and Inference*, 140(5): 1175–1181, 2010. [16](#)
- P. D. McNicholas & T. B. Murphy. Parsimonious Gaussian Mixture Models. *Statistics and Computing*, 18(3): 285–296, 2008. [2](#), [5](#), [7](#), [18](#)
- D. McParland, I. C. Gormley, T. H. McCormick, S. J. Clark, C. W. Kabudula, & M. A. Collinson. Clustering south african households based on their asset status using latent variable models. *The Annals of Applied Statistics*, 8(2): 747–767, 2014. [4](#)
- J. W. Miller & M. T. Harrison. Inconsistency of pitman-yor process mixtures for the number of components. *The Journal of Machine Learning Research*, 15(1): 3333–3370, 2014. [24](#)
- E. H. Moore. On the reciprocal of the general algebraic matrix. *Bulletin of the American Mathematical Society*, 26: 394–395, 1920. [4](#)
- K. Murphy, I. C. Gormley, & C. Viroli. *IMIFA: Infinite Mixtures of Infinite Factor Analysers and Related Models*, 2017. URL <https://cran.r-project.org/package=IMIFA>. R package version 2.0.0. [3](#), [14](#), [23](#), [24](#), [28](#), [34](#)
- R. M. Neal. Markov chain sampling methods for dirichlet process mixture models. *Journal of Computational and Graphical Statistics*, 9(2): 249–265, 2000. [9](#), [10](#)
- G. Nyamundanda, L. Brennan, & I. C. Gormley. Probabilistic principle component analysis for metabolomic data. *BMC Bioinformatics*, 11(571), 2010. [18](#)
- G. Nyamundanda, I. C. Gormley, & L. Brennan. A dynamic probabilistic principal components model for the analysis of longitudinal metabolomics data. *Journal of the Royal Statistical Society: Series C (Applied Statistics)*, 63(5): 763–782, 2014. [14](#)
- O. Papaspiliopoulos & G. O. Roberts. Retrospective Markov chain Monte Carlo methods for Dirichlet process hierarchical models. *Biometrika*, 95(1): 169–186, 2008. [10](#), [11](#), [14](#)
- P. Papastamoulis. Overfitting bayesian mixtures of factor analyzers with an unknown number of components. *Computational Statistics & Data Analysis*, 124: 220–234, 2018. [8](#), [24](#)
- D. Peel & G. J. McLachlan. Robust mixture modelling using the t distribution. *Statistics and Computing*, 10: 339–348, 2000. [24](#)
- M. Perman, J. Pitman, & M. Yor. Size-biased sampling of poisson point processes and excursions. *Probability Theory and Related Fields*, 92(1): 21–39, 1992. [2](#), [11](#)

- J. Pitman. Exchangeable and partially exchangeable random partitions. *Probability Theory and Related Fields*, 102: 145–158, 1995. [26](#)
- J. Pitman & M. Yor. The two-parameter poisson-dirichlet distribution derived from a stable subordinator. *The Annals of Probability*, 25(2): 855–900, 1997. [2](#), [9](#), [11](#)
- R Core Team. *R: A Language and Environment for Statistical Computing*. R Foundation for Statistical Computing, Vienna, Austria, 2017. [3](#), [23](#)
- A. E. Raftery, M. Newton, J. Satagopan, & P. Krivitsky. Estimating the Integrated Likelihood via Posterior Simulation Using the Harmonic Mean Identity. In *Bayesian Statistics 8*, pages 1–45, 2007. [8](#)
- S. Richardson & P. J Green. On bayesian analysis of mixtures with an unknown number of components (with discussion). *Journal of the Royal Statistical Society: Series B (Statistical Methodology)*, 59(4): 731–792, 1997. [2](#)
- J. Rousseau & K. Mengersen. Asymptotic behaviour of the posterior distribution in overfitted mixture models. *Journal of the Royal Statistical Society: Series B (Statistical Methodology)*, 73(5): 689–710, 2011. [8](#), [9](#)
- V. Ročková & E. I. George. Fast bayesian factor analysis via automatic rotations to sparsity. *Journal of the American Statistical Association*, 111(516): 1608–1622, 2016. [8](#)
- H. Rue & L. Held. *Gaussian Markov Random Fields: Theory and Applications*, volume 104 of *Monographs on Statistics and Applied Probability*. Chapman & Hall, London, 2005. [13](#)
- G. Schwarz. Estimating the dimension of a model. *The Annals of Statistics*, 6(2): 461–464, 1978. [2](#)
- L. Scrucca, M. Fop, T. B. Murphy, & A. E. Raftery. mclust 5: Clustering, classification and density estimation using Gaussian finite mixture models. *The R Journal*, 8(1): 289–317, 2016. [13](#), [18](#)
- J. Sethuraman. A constructive definition of Dirichlet priors. *Statistica Sinica*, 4: 639–650, 1994. [2](#), [10](#)
- D. J. Spiegelhalter, N. G. Best, B. P. Carlin, & A. Van Der Linde. Bayesian measures of model complexity and fit. *Journal of the Royal Statistical Society: Series B (Statistical Methodology)*, 64(4): 583–639, 2002. [2](#)
- D. J. Spiegelhalter, N. G. Best, B. P. Carlin, & A. Van Der Linde. The deviance information criterion: 12 years on. *Journal of the Royal Statistical Society: Series B (Statistical Methodology)*, 76(3): 485–493, 2014. [2](#)
- M. Stephens. Bayesian analysis of mixture models with an unknown number of components - an alternative to reversible jump methods. *The Annals of Statistics*, 28(1): 40–74, 2000. [2](#)
- M. E. Tipping & C. M. Bishop. Probabilistic principal component analysis. *Journal of the Royal Statistical Society: Series B (Statistical Methodology)*, 61(3): 611–622, 1999. [4](#), [26](#)
- R. A. van den Berg, H. C. Hoefsloot, J. A. Westerhuis, A. K. Smilde, & M. J. van der Werf. Centering, scaling, and transformations: improving the biological information content of metabolomics data. *BMC Genomics*, 7(1): 142, 2006. [18](#)

- Z. van Havre, N. White, J. Rousseau, & K. Mengersen. Overfitting bayesian mixture models with an unknown number of components. *PloS one*, 10(7): e0131739, 2015. [3](#), [8](#)
- C. Viroli. Dimensionally reduced model-based clustering through mixtures of factor mixture analyzers. *Journal of classification*, 27(3): 363–388, 2010. [2](#)
- S. G. Walker. Sampling the dirichlet mixture model with slices. *Communications in Statistics - Simulation and Computation*, 36(1): 45–54, 2007. [10](#), [11](#)
- Y. Wang, A. Canale, & D. B. Dunson. Scalable geometric density estimation. In A. Gretton & C. P. Robert, editors, *Proceedings of the 19th International Conference on Artificial Intelligence and Statistics*, volume 51 of *Proceedings of Machine Learning Research*, pages 857–865, Cadiz, Spain, 2016. PMLR. [8](#)
- M. West. Hyperparameter estimation in Dirichlet process mixture models. *ISDS discussion paper series*, pages 92–A03, 1992. [13](#), [16](#), [27](#)
- M. West. Bayesian factor regression models in the “large p, small n” paradigm. In *Bayesian Statistics 7*, pages 723–732. Oxford University Press, 2003. [23](#)
- M. J. Woo & T. N. Sriram. Robust estimation of mixture complexity. *Journal of the American Statistical Association*, 101(476): 1475–1486, 2006. [24](#)
- J. I. Yellott, Jr. The Relationship Between Luce’s Choice Axiom, Thurstone’s Theory of Comparative Judgment, and the Double Exponential Distribution. *Journal of Mathematical Psychology*, 15: 109–144, 1977. [13](#), [26](#)
- X. Yu. Gibbs Sampling Methods for Dirichlet Process Mixture Model: Technical Details. Technical report, University of Maryland, 2009. [24](#)